Dec 1, 1982

PDR

Technical Assistance for Regulatory Development:
A Simplified Repository Analysis in
A Reference Tuff Site

Malcolm D. Siegel
Margaret S. Y. Chu

Sandia National Laboratories
Albuquerque, New Mexico 87185

With Contributions From:
K. L. Erickson *
M. Reade **

*   Division 5843 Sandia National Laboratories
**   C. G. S. Inc. Urbanna, IL 61801

TABLE OF CONTENTS

ABSTRACT

Potential radionuclide releases from a hypothetical tuff repository have been calculated and compared to the limits set by the EPA Draft Standard 40CFR191. The importance of several parameters and model assumptions to the estimated discharges has been evaluated. The areas that were examined included the radionuclide solubilities and sorption, the description of the local hydrogeology and the simulation of contaminant transport in the presence of fracture flow and matrix diffusion. The uncertainties in geochemical and hydrogeological parameters were represented by assigning realistic ranges and probability distributions to these variables. The Latin Hypercube sampling technique was used to produce combinations (vectors) of values of the input variables. Groundwater flow was described by Darcy's Law and radionuclide travel time was adjusted using calculated retardation factors. Radionuclide discharges were calculated using the Distributed Velocity Method (DVM). The discharges were integrated over five successive 10,000 year periods. The degree of compliance of the repository in each scenario was illustrated by the use of Complementary Cumulative Distribution Functions (CCDF).

Our calculations suggest the following conclusions for the hypothetical tuff repository: (1) sorption of radionuclides by zeolitized tuff is an effective barrier to the migration of actinides even in the absence of solubility constraints; (2) violations of the EPA Draft standard can still occur due to discharge of ^{99}TC and ^{14}C. Retardation due to matrix diffussion, however, may eliminate discharge of these nuclides for realistic ground water flow rates; (3) in the absence of sorption by thick sequences of zeolitized tuff, discharges of U and Np under oxidizing conditions might exceed the EPA standard. Under reducing conditions, however, the low solubilities of these elements may effectively control radionuclide release.

1. INTRODUCTION

In the near future, the EPA is expected to issue 40CFR191, a draft standard for the geologic disposal of radioactive wastes. During a 180 day period, government agencies such as NRC are expected to comment on the standard. Sandia is funded by the NRC to provide information and insights useful in preparing these comments. The objective of this effort is to perform calculations similar to those performed by EPA in developing the draft standard. We have calculated integrated discharges of radionuclides in plausible scenarios. A number of media have been proposed as candidate hosts for nuclear waste repositories: bedded salt, domed salt, basalt, tuff and granite. This report documents analysis of a repository in the saturated zone of a volcanic tuff environment.

The conceptual model of the repository site is consistent with our current understanding of the characteristics of volcanic tuff environments currently being studied by the Department of Energy. It must be stressed that we have not attempted to accurately model any specific real site. At the present time the available data are not sufficient for this purpose. Large uncertainties exist in the characterization of the solubilities and sorption of radionuclides, in the description of the regional and local hydrogeology and in the mathematical treatment of contaminant transport due to fracture flow and matrix diffusion. We feel, however, that in this analysis, we have calculated reasonable upper limits of radionuclide discharge for a generic tuff repository under realistic conditions. In our calculations we have also attempted to evaluate the relative importance of the aforementioned areas of uncertainty to the estimated radionuclide release.

Appendices A through C describe in detail the assumptions and mathematical approximations that we used in our analysis. In Appendix A we discuss the data obtained from studies of Yucca Mountain at the Nevada Test Site which were used in setting realistic limits to hydrogeological parameters used in our calculations. The assumptions used to calculate hydraulic gradients for the hypothetical repository site are also discussed. In Appendix B, the geochemical environment at Yucca Mountain is described. The data which were used to estimate realistic values of radionuclide sorption ratios (R_d's or K_d's) and solubilities are also discussed. In some of our calculations we have used a retardation factor which includes the effects of matrix diffusion for ^{99}Tc, and ^{14}C and ^{129}I. Appendix C contains a derivation of the approximations we have used to adapt our one-dimensional porous media transport model to the analysis of transport in jointed porous rock.

2. GEOLOGY AND HYDROLOGY OF THE REPOSITORY SITE

2.1 Regional Geology and Hydrology

A map of the topographic setting and a regional cross-section of the repository are shown in Figures 1 and 2 respectively. The depository (point R) is located in Mountain A on the flanks of a large volcanic caldera. The depository horizon lies at a depth of approximately 3000 feet within a Tertiary volcanic tuff aquitard in the saturated zone. In Mountain A, the water table is 1500 feet below the surface and 1500 feet above the depository. The tuff aquitard is composed of layers of moderately welded to non-welded tuff units and extends several thousands of feet below the depository horizon. On a regional scale, the tuff aquitard is underlain by a Paleozoic clastic aquitard and a Paleozoic carbonate aquifer. The basal no-flow boundary of the regional groundwater system lies at the base of the carbonate aquifer.

Above the tuff aquitard lies a densely welded and highly fractured Tertiary tuff aquifer. This unit reaches a maximum thickness of about 1000 feet at Mountain A. In the washes adjacent to the mountain, the water table lies within the tuff aquifer. The piezometric surface approaches the land surface gradually along the A-D section in Figures 1 and 2; at point D water flows freely in wells at the surface.

The lateral boundaries of the regional groundwater system are approximately coincident with the edges of Figure 1. The areas north of Mesa A and Mesa B comprise the northern border of the system. The eastern and southeastern limits of the basin are marked by a series of mountains and ridges. A mountain range in the southwest marks another boundary of the system. The northwest border at the regional system is not well defined, however, the area to the west of Mesa A is known to belong to another hydrogeologic system.

Recharge to the ground water system through precipitation occurs only above the 5000 foot contour marked in Figure 1. Due to the high evaporation potential in this region, only about 15 percent of 15 inches of rainfall infiltrates to the water table in areas above this elevation. The ground water system is sluggish because of the small amount of recharge. The hydraulic gradients are low to moderate (10^{-4} to 10^{-3}) except in regions where the rocks in the saturated zone are relatively impermeable. The regional ground water flow is south-southeast through the repository and south-southwest in the southern portions of Figure 1.
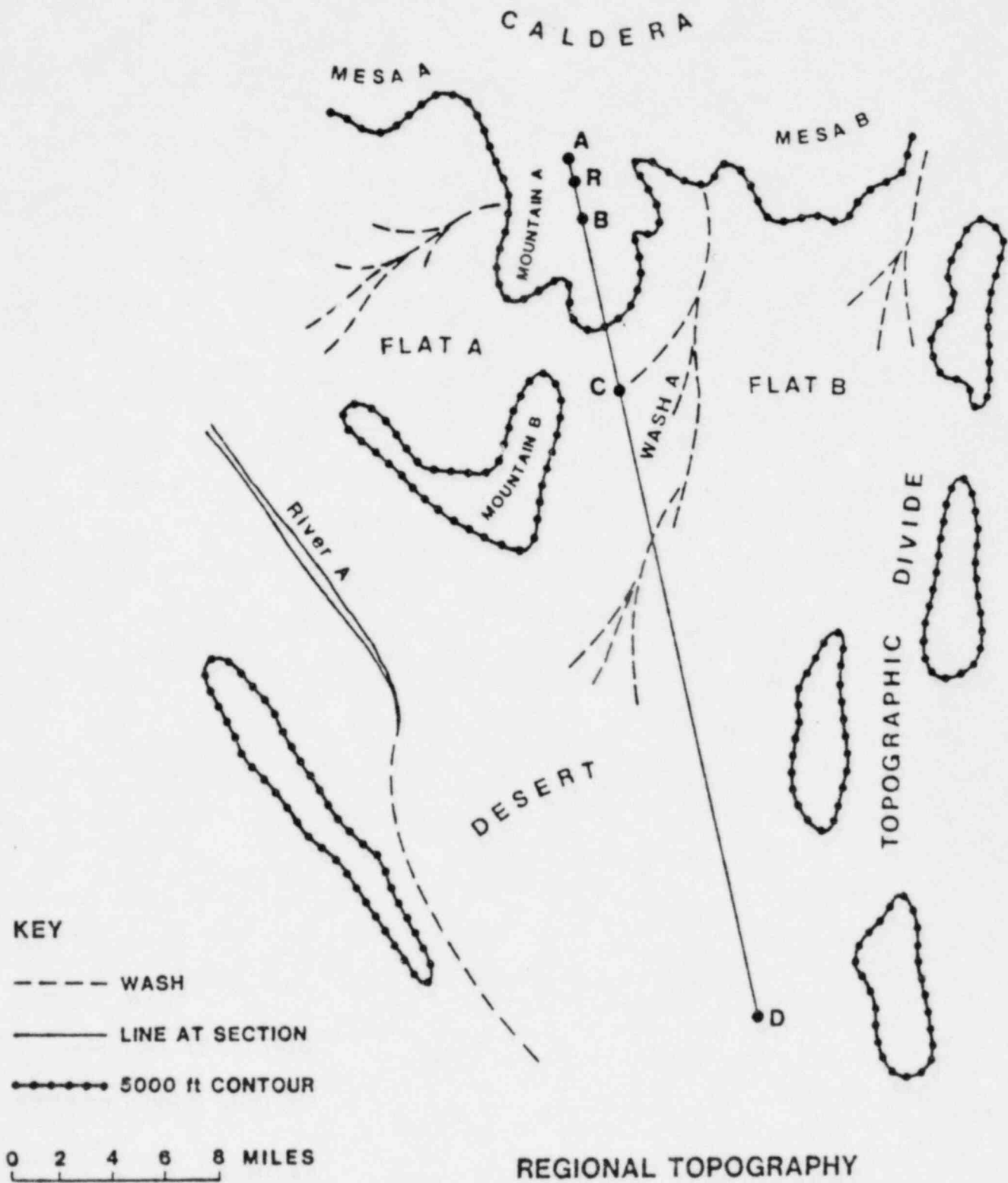
Figure 1.   Regional topography of the hypothetical tuff
            repository site
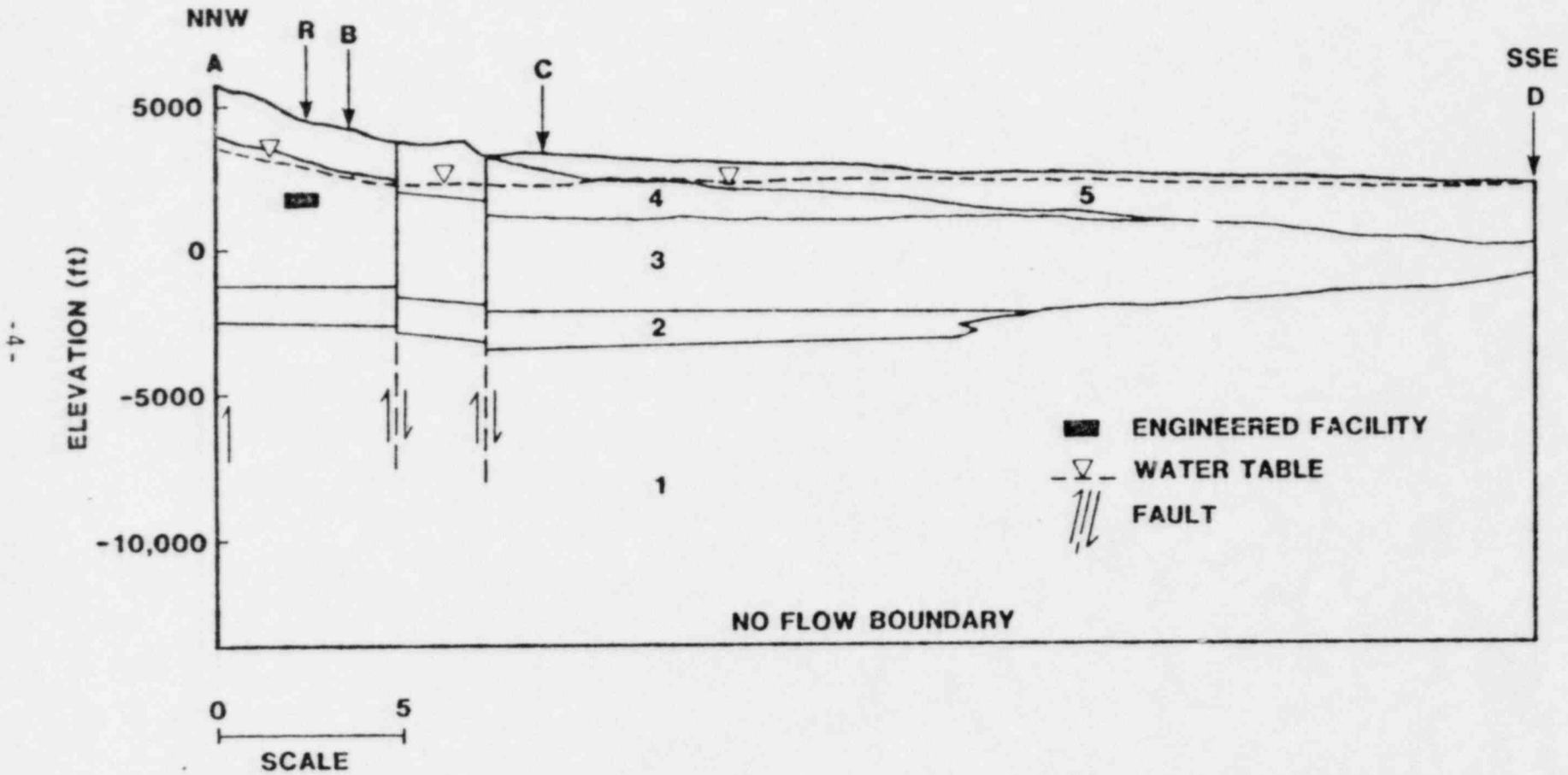
REGIONAL CROSS SECTION

Figure 2.   Regional Cross Section of Hypothetical Repository Site.

2.2 Local Geology and Hydrology

A detailed cross-section at the repository is shown in Figure 3. In Table 1, the stratigraphy for the site is described in more detail. An explanation of the petrological terms can be found in the section on Geochemistry.

In the vicinity of the volcanic caldera, the tuff layers are underlain only by granitic batholiths; all pre-existing rocks have been destroyed by volcanic eruptions. The tuff units thin with increasing distance from the volcanic centers as shown in Figure 2.

The depository is located in the middle of Unit A, a densely welded member of the tuff aquitard. This unit is a devitrified tuff, composed primarily of alkali feldspar, tridymite and cristobalite. Layer B, directly above the depository horizon, is a non-welded zeolitized tuff composed primarily of clinoptilolite. The water table lies in layer G which is similar in composition to Layer B. Layers G and I have not undergone devitrification. They have retained their original glassy nature and are designated as "vitric" in Table 1.

The geochemical and hydrological characteristics of these layers are determined primarily by the mineralogy and the degree of welding of the rocks. The local flow system and radionuclide retardation will in turn be strongly influenced by these characteristics. In Table 2, the ranges and types of distribution for several hydrogeologic parameters are described for the different types of tuff. Data from pump tests, laboratory measurements of matrix porosity of intact cores, and calculations based on fracture aperture and density were used to bound reasonable limits for hydraulic conductivity and porosity. Observations of the orientation of fractures in volcanic tuffs at the Nevada Test Site (1,2) suggest that two sets of vertical fractures dominate the joint system. In our calculations, therefore, we have assumed that values of hydraulic conductivity and effective porosity in the vertical direction are twice the values in the horizontal direction. The assumptions and methods used to delimit the range of hydraulic properties are discussed in more detail in Appendix A.

The repository site is extensively block faulted, consequently, the water table lies in the tuff aquitard near Mountain A (an uplifted block) and in the tuff aquifer beneath the adjacent washes and flats (down-dropped blocks).

Figure 3. Local Cross Section of Hypothetical Tuff Repository Site.

Table 1

STRATIGRAPHY FOR TASK III TUFF

	UNIT	DEGREE OF WELDING	ROCK TYPES	THICK NESS (FT)	COMMENT
(Tuff Aquifer)	K	NA	ALLUVIUM	60-425	
	J	DENSE	DEVITRIFIED	145	
	I	NON WELDED	VITRIC	150	
	H	DENSE	DEVITRIFIED	900	WATER TABLE AT DISTANCE=8 MILES
(Tuff Aquitard)	G	NON WELDED	ZEOLITIZED	475	WATER TABLE AT DISTANCE=0 MILES
	F	MODERATE	DEVITRIFIED	270	
	E	MODERATE	VITRIC	180	
	D	NON WELDED	ZEOLITIZED	150	
	C	DENSE	DEVITRIFIED	250	
	B	NON WELDED	ZEOLITIZED	300	
	A	DENSE	DEVITRIFIED	400	DEPOSITORY HORIZON
		MODERATE	ANALCIME	270	

Table 2

RANGES OF HYDROGEOLOGIC PARAMETERS

Parameter	Densely Welded Tuff	Moderately Welded Tuff	Non-Welded Tuff
Horizontal hydraulic conductivity (ft/day)''	2×10^{-5}-30 (LU)'	3×10^{-5}-5 (LN)	10^{-5}-2 (LN)
Horizontal effective porosity (%)''	4.4×10^{-4}-0.32 (LN)	0.03-22 (LU)	20-48 (N)
Horizontal hydraulic gradient	1×10^{-3}-1×10^{-1} (LU)	1×10^{-3}--1×10^{-1} (LU)	1×10^{-3}-1×10^{-1} (LU)
Vertical hydraulic gradient	1×10^{-2}-4×10^{-2} (U)	1×10^{-2}-4×10^{-2} (U)	1×10^{-2}-4×10^{-2} (U)
Grain density (gm/cm^3)	2.3	2.2	1.7
Horizontal fracture porosity''(%)	4.4×10^{-4}-0.32	0.0-0.06	---
Total Porosity (%)	3-10	10-38	20-50

' Type of distribution is indicated in parenthesis: (LU)-log uniform; (LN)-lognormal; (U)-uniform.

'' Values of these properties in the vertical direction are 2x the values in the horizontal direction.

The water table in the vicinity of the repository is indicated in Figure 3. Near Mountain A, the piezometric surface lies within Unit H and parallels the top of this layer. The horizontal hydraulic gradient near the repository lies within the range 10^{-1} to 10^{-3}. Approximately 2 miles from the repository, the water table enters the tuff aquifer (in Layer H) and the gradient decreases to 10^{-2} to 10^{-4}. This "hinge effect" is due to the combined effects of stratigraphy, contrasts in hydraulic conductivity and increased recharge at elevations above 5000 feet. In our calculations, however, we have sampled the horizontal gradient over a range of 10^{-1} to 10^{-3} for conservatism.

The blocks faulting can create local abrupt changes in head at vertical faults where relatively permeable water-bearing zones are abutted against impermeable layers. For the purpose of our calculations, however, we have ignored these local hetero-geneities. The water lies more than 1000 feet below the sur-face at all points along section ARBC. Local changes in the water table will not substantially affect radionuclide trans-port on the scale of our model; the water table, therefore, is represented by straight lines in Figure 3.

In all of the release scenarios (except scenarios 2 and 2B) we have assumed that radionuclides travel vertically from the engineered facility to the water table under the influence of thermal buoyancy related to the heat generated by the emplaced waste. We have also assumed that the volume of annual ground water flow through the repository is not large enough to appre-ciably perturb the regional flow system. Supply of ground water to the repository will be sufficient to saturate the repository at all times during the 50,000 year period of inter-est. This assumption adds another element of conservatism to our calculations and will be discussed further in Appendix A.

3. WASTE AND REPOSITORY DESCRIPTION

3.1 Waste

The inventory (Table 2) assumed in this work is equal to half the projected accumulation of 10-year-old spent fuel in the United States by the year 2010. This would contain a total of 103,250 BWR and 60,500 PWR assemblies; a total of 46,800 metric tons of heavy metal (MTHM). All radionuclides specified in the Release Limit Table of the EPA Standard are included in this inventory list.

Based on the inventory and toxicity of each radionuclide the following chains of radionuclides were considered:

(1) $^{240}Pu \rightarrow {}^{236}U \rightarrow {}^{232}Th \rightarrow {}^{228}Ra$

(2) $^{245}Cm \rightarrow {}^{241}Pu \rightarrow {}^{241}Am \rightarrow {}^{237}Np \rightarrow {}^{233}U \rightarrow {}^{229}Th$

(3) $^{246}Cm \rightarrow {}^{242}Pu \rightarrow {}^{238}U \rightarrow {}^{234}U \rightarrow {}^{230}Th \rightarrow {}^{226}Ra$

$$^{238}Pu \longrightarrow {}^{234}U \qquad\qquad {}^{226}Ra \downarrow {}^{210}Pb$$

(4) $^{243}Am \rightarrow {}^{239}Pu \rightarrow {}^{235}U \rightarrow {}^{231}Pa \rightarrow {}^{227}Ac$
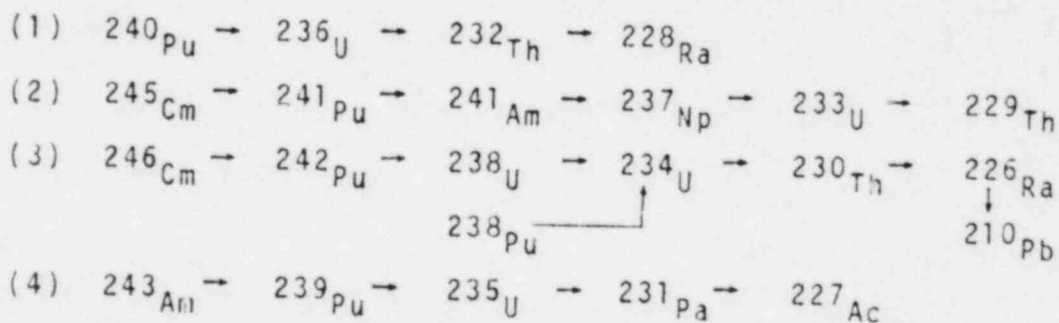
The fission and activation product radionuclides ^{99}Tc, ^{129}I, ^{126}Sn, ^{90}Sr, ^{14}C, ^{135}Cs, and ^{137}Cs were also considered in this work.

All canisters containing the wastes are assumed to have a life of 1,000 years after emplacement. At year 1,000, all canisters fail simultaneously and radionuclide release begins. Radionuclide release is assumed to be determined by a constant rate of breakdown of the waste form. The waste matrix is assumed to dissolve at an annual rate of 10^{-3} to 10^{-7} of the original mass. Radionuclides are assumed to be uniformly distributed throughout the matrix so that their release rate is directly proportional to the matrix dissolution rate.

3.2 Subsurface Facility

The reference subsurface facility is a mined facility at a depth of 3,000 feet below the surface. A description of the facility is summarized in the following table.

Areal dimensions -- 2,000 acres ($8.71 \times 10^7 \text{ft}^2$)
(Reference 3, Table C1)

Height = 23 ft.
Rep. Volume = $8.71 \times 10^7 \times 23 = 2.0 \times 10^9 \text{ft}^3$

Extraction Ratio = 20% (Reference 3, p. 88)
Porosity of Backfill = 20%

* Porosity volume of depository = $8.0 \times 10^7 \text{ft}^3$

Table 3

INVENTORY OF REFERENCE REPOSITORY
(SPENT FUEL FROM 46,800 MTHM)

Radionuclide	Half Life	Curies
Pu240	6.76E3	2.1E7
U236	2.39E7	1.0E4
Th232	1.41E10	1.7E-5
Ra228	6.7	4.7E-6
Cm245	8.27E3	8.4E3
Pu241	14.6	3.2E9
Am241	433.	7.5E7
Np237	2.14E6	1.5E4
U233	1.62E5	1.8
Th229	7300.	1.3E-3
Cm246	4710.	1.6E3
Pu242	3.79E5	7.5E4
U238	4.51E9	1.5E4
Pu238	89.	9.4E7
U234	2.47E5	3.5E3
Th230	8.E4	0.19
Ra226	1600.	3.5E-4
Pb210	21.	3.3E-5
Am243	7650.	6.6E5
Pu239	2.44E4	1.4E7
U235	7.1E8	7.5E2
Pa231	3.25E4	0.25
Ac227	21.6	5.2E-2
Tc99	2.14E5	6.1E5
I129	1.6E7	1.5E3
Sn126	1.0E5	2.2E4
Sr90	28.9	2.4E9
C14	5730.	3.5E4
Cs135	2.0E6	1.3E4
Cs137	30.	3.5E9

4. SITE GEOCHEMISTRY AND RADIONUCLIDE RETARDATION

4.1 Geochemical Environment of the Hypothetical Tuff Site

The migration rate of radionuclide in the tuff repository site will depend on the interactions between the dissolved species and the rock matrix and between the different aqueous species in the liquid phase. Important geochemical parameters which must be characterized include the major and minor element composition, pH, Eh, and temperature of the ground water and the mineralogy of tuff layers through which the radionuclides migrate.

The lithology of each tuff unit in our hypothetical tuff site is described in Table 1. They are classified as zeolitized, vitric or devitrified. A more detailed discussion of the mineralogy may be found in Appendix B. The ground water in the repository site is assumed to be a sodium-potassium-bicarbonate water similar to that described by Winograd and Thordarson (4) at the Nevada Test Site. The Eh is assumed to be mildly oxidizing and the pH are between 7.2 and 8.3. The chemical composition of water from the vicinity of Yucca Mountain and the justification for the above assumptions are described in detail in Appendix B. The temperature assumed in the transport legs in the far field of the repository site is between 30 and 40°C. This range is based on the geothermal gradient at Yucca Mountain.

4.2 Sorption Ratios

The sorption ratio (R_d) is an experimentally determined ratio of the amount of radionuclide bound to a solid phase to the amount of nuclide in a volume of liquid in contact with the solid.

$$R_d \text{ (ml/gm)} = \frac{\text{gm radionuclides per gm rock}}{\text{gm radionuclide per ml water}}$$

Values for ranges of R_d for the different types of tuff found in the reference repository are given in Table 4. These ranges are based primarily on a review of the results of sorption ratio studies by scientists at Los Alamos Laboratories (5-10).

The degree of conservatism for these ranges is discussed in Appendix B. Elements for which no sorption data are published are enclosed in brackets in Table 4. They have been assigned to R_d values of chemical homologs for which data are available (11). To our knowledge, there are no acceptable data for

Table 4

RANGES OF R_d (ml/gm) VALUES SAMPLED BY LHS

Element	Vitric Tuff	Devitrified Tuff	Zeolitized Tuff with Clinoptilolite
Sr, [Ra, Pb, Sn]	117-300	50-450	290-213,000
Cs	429-8600	120-2000	615-33,000
Pu	70-450	80-1400	250-2000
Am, [Cm, Pa, Th, Ac]	85-360	190-4600	600-9500
Np	5-7	5-7	4.5-31
U	0-11	1-14	5-15
I, ^{14}C	0	0	0
Tc	0-2	0.3-1.2	0.15-2.0

Np sorption on vitric tuff; the sorption ratio range for devitrified tuff was assigned to this media.

4.3 Solubility Limits of Radionuclides

The solubility limits that were assigned to each element in this study are listed in Table 5. The values in this table are probably upper bounds for the solubilities of these elements in a volcanic tuff environment. The determination of solubilities of radionuclides in ground water associated with a repository in tuff requires experimental studies and calculations describing the possible interactions between nuclides and ligands over a range of temperatures, water compositions and redox conditions. The theoretical calculations are not within the scope of this contract and to our knowledge have not been carried out. Few experimental data describing radionuclide solubility in tuff are available at this time. Due to the time constraints of this contract, we have compiled this list of solubility values from a limited amount of experimental data and solubilities calculated from a limited review of thermochemical data (12-16). A discussion of the conservatism of these data may be found in Appendix B.

4.4 Radionuclide Retardation

The classical expression for retardation in porous media was used for layers of zeolitized tuff in all scenarios.

$$R = 1 + R_d \cdot \rho \cdot \frac{(1 - \phi)}{\phi} \qquad (4.1)$$

Where ϕ is the effective porosity of the rock
        ρ is the grain density of the rock
        R_d is the radionuclide sorption ratio (ml/gm)

The calculation of retardation in moderately and densely welded tuff layers was different in each scenario. Detailed descriptions of the scenarios are found in the next section. In scenarios 3 and 4, expression 4.1 was used for moderately welded tuff layers. It was assumed that all radionuclides were unretarded in densely welded layers in scenarios 1, 3, 4, 5, and 6. In scenarios 1, 5, and 6 it was assumed that all radionuclides were unretarded in moderately welded tuff layers also.

Table 5

ELEMENT SOLUBILITIES USED IN
MIXING CELL CALCULATIONS

Element	Solubility gm/gm	Reference
Pu	2.4×10^{-4}	*
U	2.4×10^{-5}	15
Th	2.3×10^{-7}	13
Ra	2.3×10^{-8}	16
Cm	2.5×10^{-11}	*
Am	2.4×10^{-12}	15
Np	2.4×10^{-8}	15
Pb	2.1×10^{-6}	*
Pa	2.3×10^{-2}	13
Ac	no limit	*
Tc	no limit	*
I	no limit	*
Sn	1×10^{-3}	13
Sr	2×10^{-6}	13,16
Cs	no limit	*
C	3×10^{-5}	*

*   See discussion in Appendix B

In scenarios 1B, 2, 2B, and 5B matrix diffusion for Tc, ^{14}C, and I was included explicitly in the calculations of radionuclide retardation:

$$R = 1 + \phi_m \cdot \left(\frac{1-\epsilon}{\epsilon} \right) \quad \cdot \quad \left(1 + R_d \cdot \rho \cdot \left(\frac{1-\phi_m}{\phi_m} \right) \right) \qquad (4.2)$$

Where ϕ_m = matrix porosity
   ϵ = fracture porosity
   ρ = grain density of rock matrix
   R_d = radionuclide sorption ratio (ml/gm)

The derivation of this expression and constraints on its use are discussed in Appendix C.

5. GROUNDWATER TRANSPORT MODEL

In the calculations of radionuclide transport it is assumed that groundwater flow is described by Darcy's Law:

$$q = Q/A = KI \tag{5.1}$$

where Q is the volumetric flow rate through an area A, normal to the flow direction, I is the hydraulic gradient, K is the hydraulic conductivity, and q is the Darcy velocity. When the flow passes through a series of layers with different hydraulic properties, an "effective" hydraulic conductivity may be calculated by

$$K = \frac{\sum_i L_i}{\sum_i \frac{L_i}{K_i}} \tag{5.2}$$

with

L_i = thickness of layer i

K_i = hydraulic conductivity of layer i

The total groundwater travel time is given by

$$Time = \sum_{i=1} \frac{L_i}{V_i} \tag{5.3}$$

where V_i is the interstitial groundwater velocity in layer i and is equal to q/ϕ_i, with ϕ_i being the effective porosity of layer i. We have assumed that ϕ_i and K_i are correlated with $r^2 = 0.70$. The geometry of the flow path is described for each scenario in Section 6.

When a radionuclide (RN) is transported by ground water, the radionuclide travel time (T_{RN}) is increased by its retardation factor. This is given by

$$T_{RN} = \sum_i \frac{L_i \cdot R_i^{RN}}{V_i} \tag{5.4}$$

where Ri^{RN} is the retardation factor of radionuclide RN in layer i.

The Distributed Velocity Method (DVM) (17) has been developed by Sandia to simulate long chains of radionuclides transported by ground water. In this study we calculated the average velocity of radionuclides using Equation (5.4). The DVM code was then used to calculate the discharges of radionuclides.

6. DESCRIPTIONS OF SCENARIOS AND CALCULATIONS

6.1 Introduction

The conceptual model of our hypothetical repository site is consistent with our current understanding of the characteristics of volcanic tuff environments being studied by the Department of Energy. We have not attempted to accurately model any particular real site; at the present time the available data are not sufficient for this purpose. Large uncertainties exist in the characterization of the solubilities and sorption of radionuclides, in the description of the regional and local hydrogeology and in the mathematical treatment of contaminant transport in the presence of fracture flow and matrix diffusion. In our calculations, we have attempted to evaluate the relative importance of these areas of uncertainty to the estimated radionuclide discharge. We have calculated radionuclide release for several scenarios using different combinations of the following assumptions:

A. Release rate of radionuclides from the engineered facility
   1. limited by leach rate
   2. solubility limited

B. Representation of retardation of radionuclides in moderately welded units
   1. no retardation
   2. porous media approximations with zeolite R_d's
   3. porous media approximations with R_d's for vitri. or devitrified tuff

C. Matrix diffusion
   1. no credit given for retardation
   2. calculation of retardation of ^{99}Tc, ^{129}I, and ^{14}C in welded units

D. Distance to accessible environment
   1. one mile
   2. eight miles

E. Flow path
   1. vertical path and gradient controlled by thermal pulse
   2. horizontal migration only

F. Location of water table
   1. in zeolitized tuff
   2. in densely welded tuff (300 ft above present day level)

-20-

The characteristics of each scenario are summarized in
Table 6. The release rate of radionuclides from the engineered
facility was set equal to the leach rate (10^{-3} to 10^{-7} of
the original inventory) in all scenarios except scenario 2B.
The mixing cell option of NWFT/DVM was used in the scenario 2B
and will be described in more detail in Section 6.5.

The uncertainties in geochemical and hydrogeological parameters
were represented by assigning realistic ranges and probability
distributions to these variables. The Latin Hypercube Sampling
Technique (18) was used to produce 105 combinations (vectors)
of values of the input variables. Integrated radionuclide dis-
charges for five successive 10,000 year periods were calculated
as described in Section 5. A release ratio was calculated for
each vector by dividing the magnitude of the discharge of each
radionuclide by the corresponding EPA release limit (19) and
then summing over all radionuclides. The results are presented
as probability distributions of the release ratios for each
scenario (Complementary Cumulative Distribution Functions)
(6). The curve indicates the ability of the repository site to
limit the release of radionuclides. They also illustrate how
our ability to assess the compliance of a repository with the
EPA Draft Standard is affected by the uncertainty in the input
data.

We have not made quantitative estimates of the probability of
occurrence of any of the scenarios. We have assumed only that
each of the scenarios is an "anticipated event" (corresponding
to a "reasonably foreseeable release" in the EPA Draft Standard
(19)). We feel that the scenarios have a reasonable probabil-
ity of occurrence within the 10,000 year regulatory period.

The water table is at least 1,000 feet below the land surface
at all points within the hypothetical repository site of our
analyses. All of the scenarios require that a well be drilled
at least to the depth of the water table and that the radio-
nuclides are withdrawn continuously for 10,000 years or lon-
ger. We have based our subjective estimate of the probability
of drilling at the hypothetical tuff site on estimates of the
water, hydrocarbon and heavy metal ore potential of the Nevada
Test Site. Our estimate of the probability of a pluvial period
and subsequent rise in the water table at the repository site
(Scenario 5) is based on information concerning past climatic
changes at NTS.

Table 6

DESCRIPTIONS OF SCENARIOS

| SCENARIO | DISTANCE BETWEEN DEPOSITORY AND POINT OF DISCHARGE | | REPRESENTATION OF RETARDATION IN WELDED UNITS | | | | VERTICAL GRADIENT CONTROLLED BY THERMAL PULSE | | CLIMATIC CHANGE CAUSES 300 FT RISE IN WATER TABLE | |
| | | | DENSELY AND MODERATELY WELDED | | MODERATELY WELDED ONLY | | | | | |
	1 MILE PUMP	8 MILE PUMP	MATRIX DIFFUSION MODEL	FRACTURED MEDIUM WITH NO RETARDATION	POROUS MEDIUM WITH ZEOLITES	POROUS MEDIUM WITH DEVITRIFIED TUFF OR VITRIC TUFF	YES	NO	YES	NO
#1	X			X			X			X
#1B	X		X				X			X
#2	X		X					X		X
#2B	X		X					X		X
#3	X				X		X			X
#4	X					X	X			X
#5	X			X			X		X	
#5B	X		X				X		X	
#6		X		X			X			X

* Scenarios 2 and 2B differ from each other in their treatment of the source term. Scenario 2 was a leach limited source term with no solubility limits. In scenario 2B we used the mixing cell option of NWFT/DVM which allows solubility limits to constrain the rate of radionuclide release from the repository.

-22-

6.2   Scenarios 1, 3, 4, and 1B: Alternate representations of
      retardation in welded tuff layers

Scenario 1 - The "Base Case"

Scenario 1 can be considered the base case scenario in our
analyses of the hypothetical tuff site (Figure 4).   The major
geological barriers to radionuclide migration are the layers of
zeolitized tuff above the repository.   The magnitude of the
vertical hydraulic gradient is determined by a buoyancy effect
of water heated by the repository as described in Appendix A.
Ground water and radionuclides from the repository will travel
along the vertical gradient to the top of the water table then
migrate horizontally down the horizontal hydraulic gradient.
The horizontal gradient is calculated as the sum of the
regional gradient plus a component related to the upwelling
heated water from the repository.

At a distance of one mile from the repository, a well pumps
water from this upper saturated unit.   The major barrier to
horizontal transport of the radionuclide is retardation in the
zeolitized layer G.   Layers of zeolitized tuff are treated as
porous media in the fluid transport and retardation calcula-
tions.   Layers of moderately or densely welded tuff are treated
as porous media in the transport calculations but it is assumed
that no retardation occurs in these layers.   Since no credit is
given to retardation in the welded units, the calculated dis-
charge is an upper bound for release associated with the fluid
transport path described above.

Scenarios 3 and 4 -Porous media approximations for moderately
welded tuff layers

Scenarios 3 and 4 differ from scenario 1 only in the treatment
of retardation in the moderately welded tuff layers (Figures 5
and 6).   In both scenarios these layers are treated as porous
media.   Moderately welded tuffs are characterized by physical
and chemical properties that are intermediate between densely
welded devitrified tuffs and nonwelded zeolitized tuffs.   In
scenario 3, R_d values of zeolitized tuff (Table 4) are used
to calculate retardation factors.   These calculations provide a
lower bound to discharge from the site for scenarios 1, 3, and
4. R_d values for vitric tuffs and devitrified tuffs are used
to calculate retardation in layers E and F respectively in sce-
nario 4.   Values of all other variables are the same as in cor-
responding vectors of scenario 1.

Scenario 1B - Matrix diffusion in welded tuff layers

Scenario 1B (Figure 7) differs from scenario 1 only by the inclusion of matrix diffusion in calculations of radionuclide retardation in moderately and densely welded tuff layers. The calculation of a retardation factor which includes the effects of matrix diffusion has been described in Equation 4.2 and in Appendix C. At present, it can only be shown that this expression is valid for radionuclides with R_d = 0 (K. Erickson, personal communication). For scenario 1B, therefore, retardation due to matrix diffusion was considered only for ^{129}I, ^{99}Tc and ^{14}C (see Table 4).

Results

Radionuclide discharge rates for each vector were calculated. Discharge rates were integrated for 10,000 year periods from 0 to 50,000 years. The results of the calculations are presented as complementary cumulative distribution functions for each 10,000 year period in Figures 8A-8E. (20) The number of vectors that violate the EPA Standard, the maximum violation and the sum of the release ratio over all vectors are presented in Table 7. For these scenarios, all violations of the EPA Standard are due to discharges of ^{99}Tc and ^{14}C. The effect of retardation in the moderately welded units on the integrated discharge can be assessed by comparing the values for scenarios 3 and 4 to corresponding values for scenario 1. It can be seen that discharge is decreased for the first 40,000 years and increased in the period from 40,000 to 50,000 years relative to scenario 1. Comparison of the results for scenario 1B with those for scenario 1 shows that although discharge of the radionuclides is decreased significantly by matrix diffusion, violations of the EPA release limit still occur.

The characteristics of the three vectors whose radionuclide discharges violate the EPA Standard are shown in Table 8. When these values of hydraulic gradient and darcy velocity are compared to the ranges of hydrogeologic parameters sampled by the LHS for input, it can be seen that the high radionuclide discharges are due primarily to large groundwater fluxes. These annual groundwater discharges range from 2 percent to 7 percent of the present day recharge of the Pahute Mesa groundwater system at the Nevada Test Site (21, 22). In Appendix A it is shown that this fraction is unrealistically high for Yucca Mountain. Therefore, we can conclude that violation of the EPA Standard for a groundwater flow path similar to Scenario 1B is very unlikely.
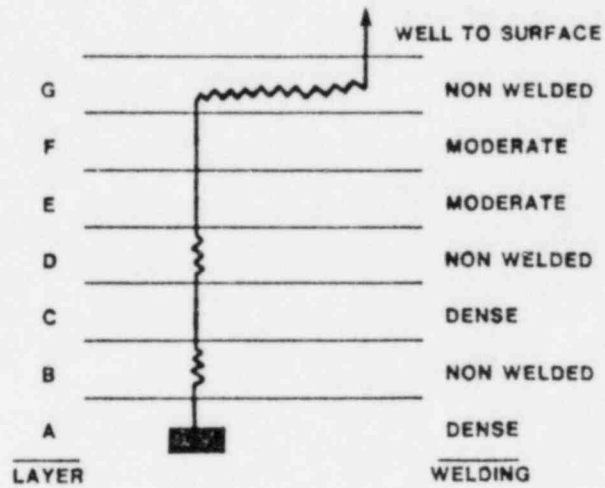
SCENARIO 1

1 mile well; moderate = fractured; thermal buoyancy; no pluvial

LEG	LAYERS	WELDING - RETARDATION	LENGTH (ft)	
1	A	dense - no retardation	200	v
2	B	nonwelded - porous - zeolites	300	v
3	C	dense - no retardation	250	v
4	D	non-welded - porous - zeolites	150	v
5	E	moderate - no retardation	180	v
6	F	moderate - no retardation	270	v
7	G	nonwelded - porous - zeolites	5280	h

FLOW PATH

LAYER		WELDING
		WELL TO SURFACE
G		NON WELDED
F		MODERATE
E		MODERATE
D		NON WELDED
C		DENSE
B		NON WELDED
A		DENSE

KEY

▨ DEPOSITORY

☐ LAYERS WITH NO RETARDATION

[§] LAYERS WITH RETARDATION

Figure 4

SCENARIO 3

1 mile well; moderate = porous zeolite; thermal buoyancy; no pluvial

LEG	LAYERS	WELDING - RETARDATION	LENGTH (ft)	
1	A	dense - no retardation	200	v
2	B	nonwelded - porous - zeolites	300	v
3	C	dense - no retardation	250	v
4	D	non-welded - porous - zeolites	150	v
5	E	moderate - porous - zeolite	180	v
6	F	moderate - porous - zeolite	270	v
7	G	nonwelded - porous - zeolites	5280	h

FLOW PATH

LAYER		WELDING
G		NONWELDED
F		MODERATE
E		MODERATE
D		NONWELDED
C		DENSE
B		NONWELDED
A		DENSE

WELL TO SURFACE

Figure 5

-26-
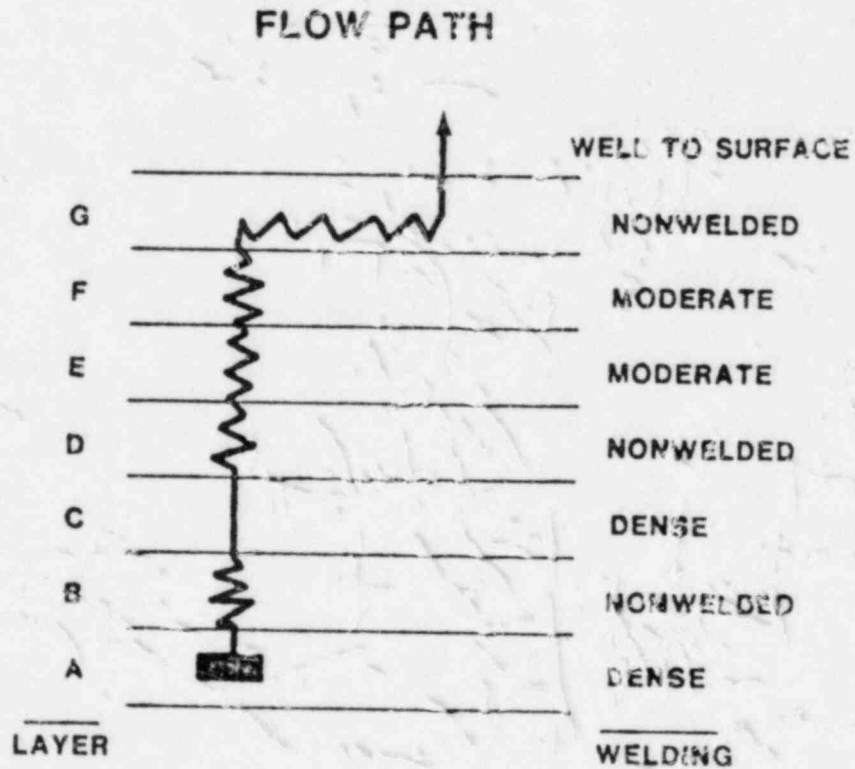
SCENARIO 4

1 mile well; moderate = porous, vitric or devitrified tuff, thermal buoyancy

LEG	LAYERS	WELDING - RETARDATION	LENGTH (ft)	
1	A	dense - no retardation	200	v
2	B	nonwelded - porous - zeolites	300	v
3	C	dense - no retardation	250	v
4	D	non-welded - porous - zeolites	150	v
5	E	moderate - porous - vitric	180	v
6	F	moderate - porous - devitrified	270	v
7	G	nonwelded - porous - zeolites	5280	h

FLOW PATH
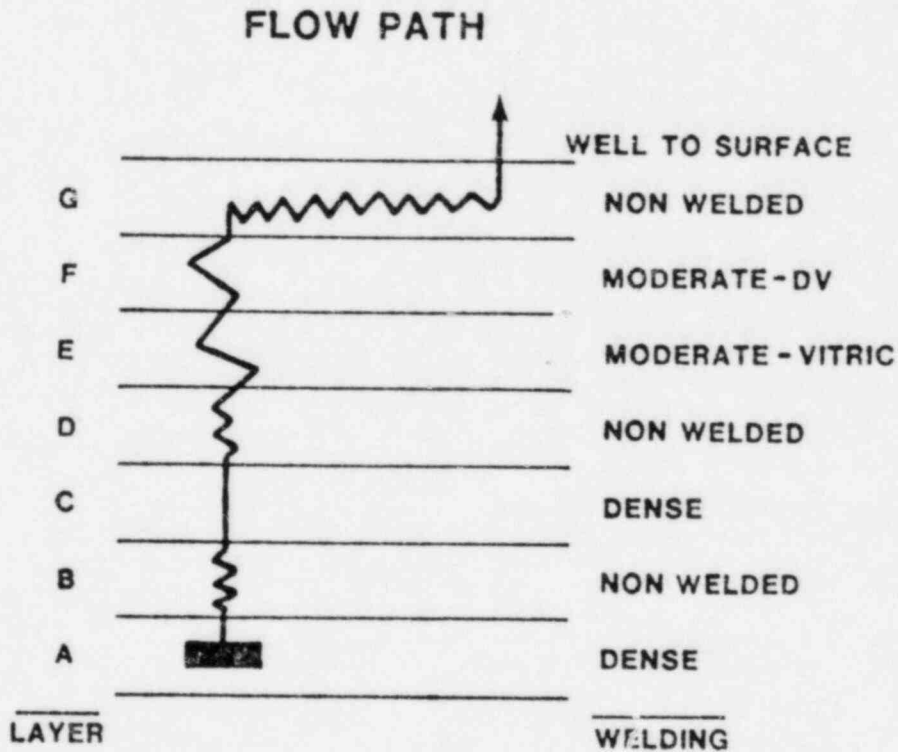
Figure 6

SCENARIO 1B

1 mile well; matrix diffusion; thermal buoyancy no pluvial

LEG	LAYERS	WELDING - RETARDATION	LENGTH (ft)	
1	A	dense - matrix diffusion	200	v
2	B	nonwelded - porous - zeolites	300	v
3	C	dense - matrix diffusion	250	v
4	D	non-welded - porous - zeolites	150	v
5	E	moderate - matrix diffusion	180	v
6	F	moderate - matrix diffusion	270	v
7	G	nonwelded - porous - zeolites	5280	h

FLOW PATH

KEY
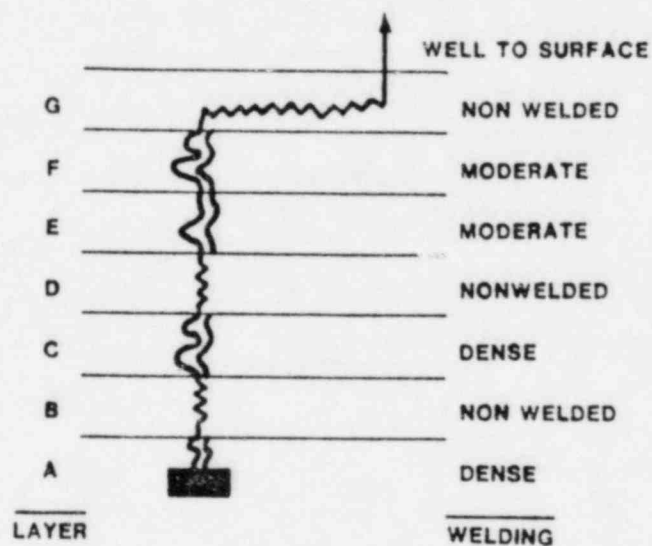
DEPOSITORY

LAYERS WITH MATRIX DIFFUSION

LAYERS WITH RETARDATION (POROUS MEDIA)

Figure 7
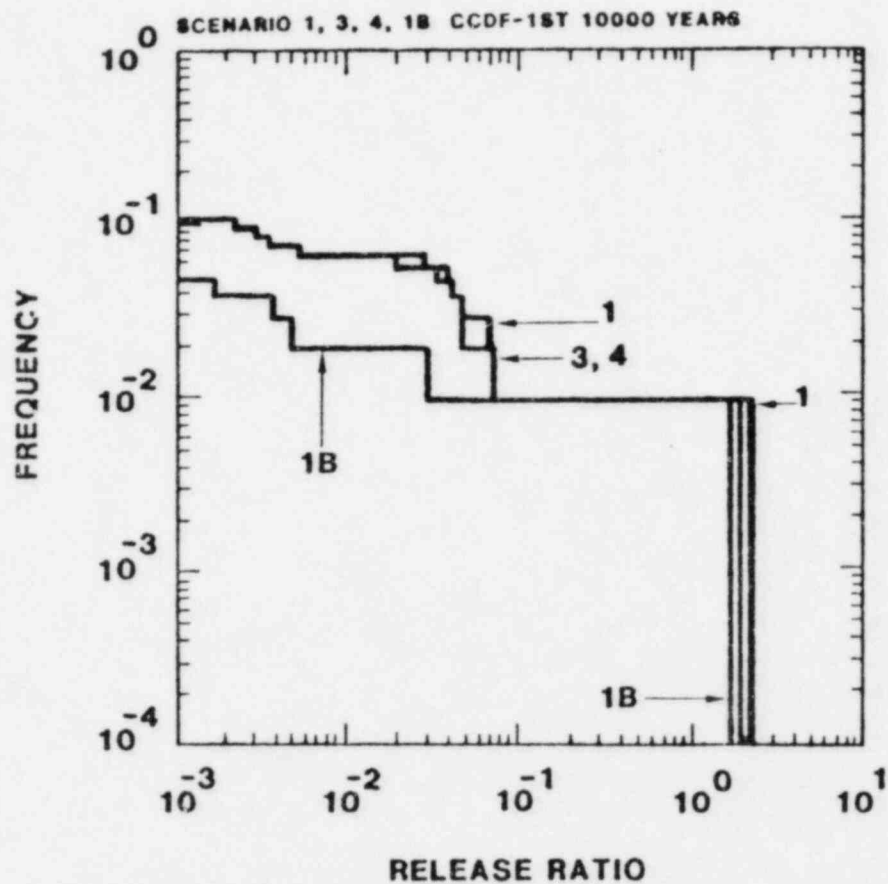
-28-

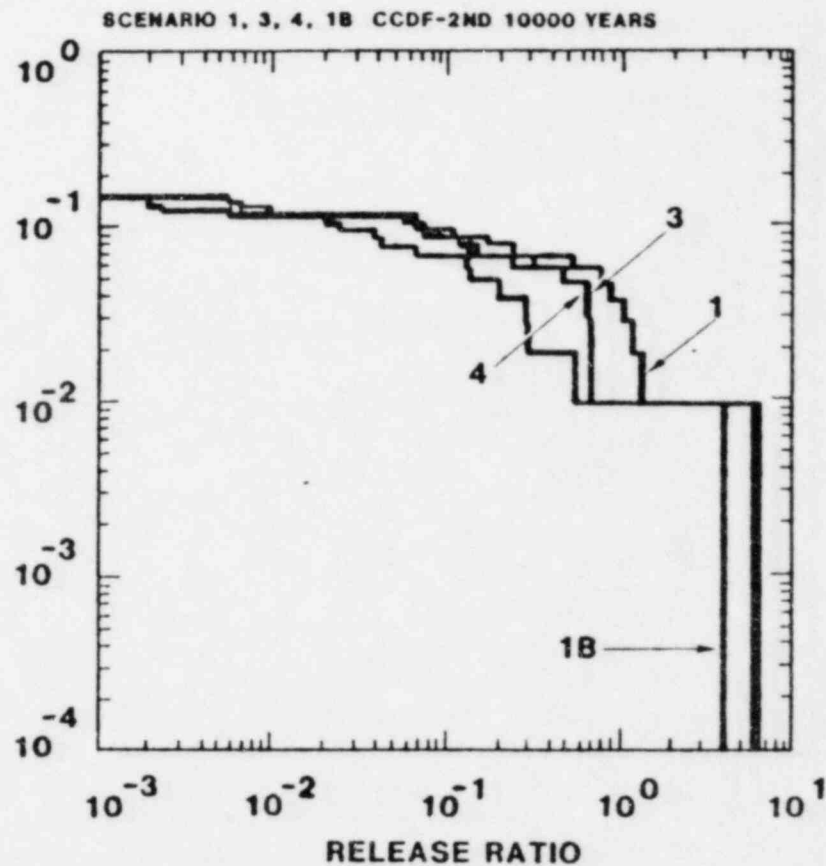Figure 8.a   Figure 8.b

Figure 8.   Complementary Cumulative Distribution Functions for Scenarios 1, 1B, 3, and 4:
            Alternate Representations of Retardation in Welded Tuff Units.

        1 = base case; 1B = base case with matrix diffusion; 3 = zeolites;
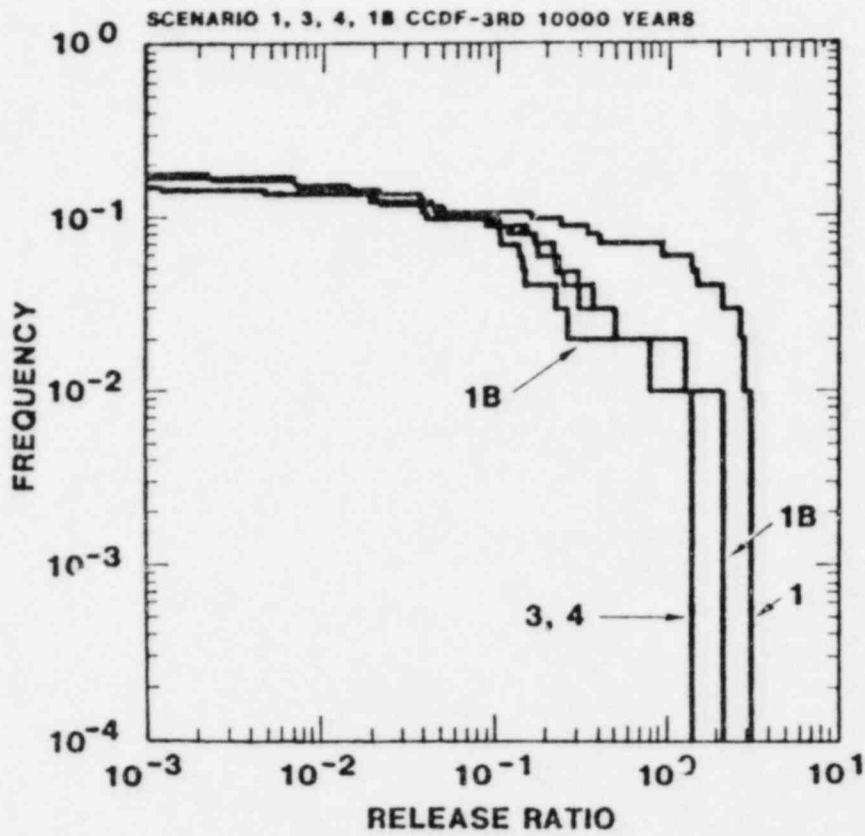   4 = vitric or devitrified

SCENARIO 1, 3, 4, 1B CCDF-3RD 10000 YEARS

SCENARIO 1, 3, 4, 1B CCDF-4TH 10000 YEARS
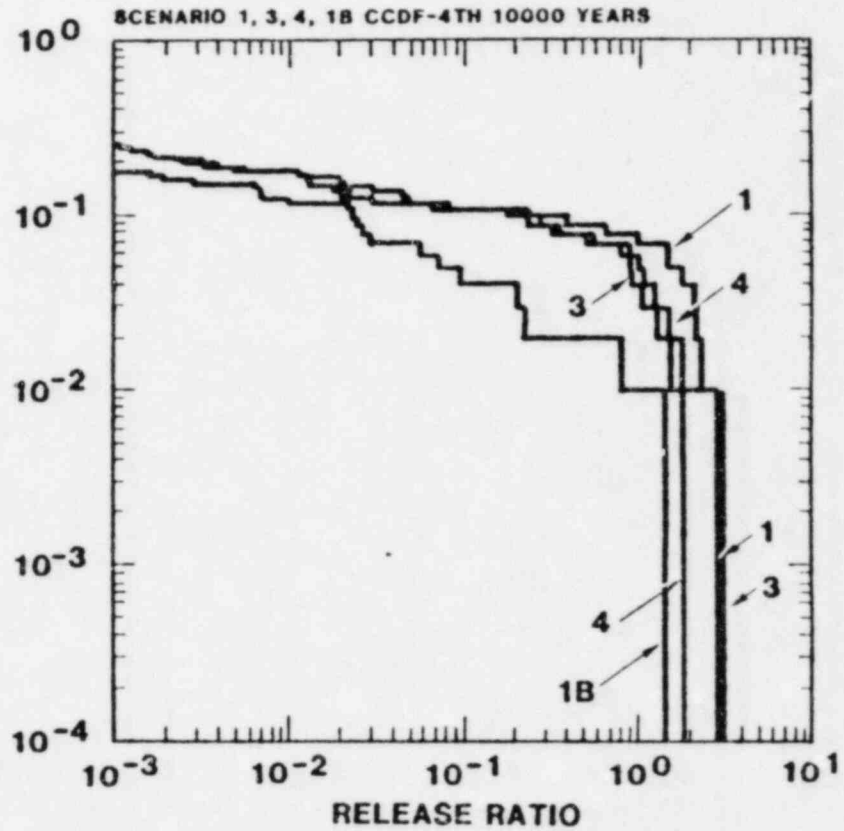
Figure 8.c

Figure 8.d
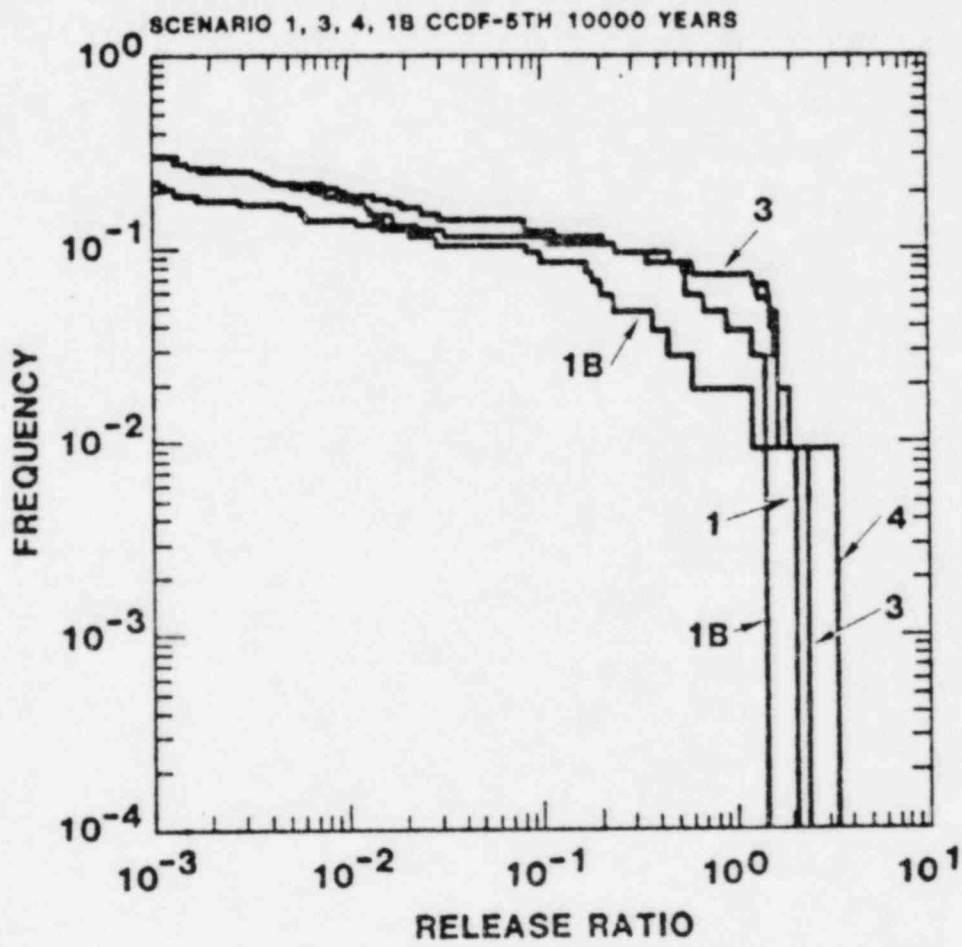
SCENARIO 1, 3, 4, 1B CCDF-5TH 10000 YEARS

Figure 8.e

Table 7

NUMBER OF VIOLATING VECTORS, MAXIMUM OF RELEASE RATIOS AND SUM OF RELEASE RATIOS
OVER ALL VECTORS FOR EACH 10,000 YEAR PERIOD

Scenario	0-10,000yr	10,000-20,000yr	20,000-30,000yr	30,000-40,000yr	40,000-50,000yr
1	1*	4	7	8	4
	2.4**	5.9	3.1	2.9	2.0
	2.5***	12.1	16.5	17.0	10.7
3	1	1	1	4	8
	1.9	6.2	1.4	3.1	2.3
	2.2	10.2	4.8	12.0	14.4
4	1	1	1	6	8
	1.9	6.1	1.4	1.5	3.4
	2.1	10.1	4.6	10.6 ·	15.6
1B	1	1	2	1	2
	1.7	3.9	2.2	1.5	1.5
	1.8	5.7	5.0	3.1	5.2

*   number of violating vectors
**   maximum release ratio
***   sum of release ratios

- 32 -

Table 8

PROPERTIES OF VECTORS WHICH VIOLATE EPA STANDARD
IN SCENARIO 1B

VECTOR	3	24	51
PARAMETER			
Maximum R* for Tc	10827	7570	14364
Average vertical darcy velocity (ft/yr)	0.32	0.13	0.41
Vertical hydraulic gradient	0.04	0.03	0.03
Average horizontal darcy velocity (ft/yr)	0.17	0.88	0.36
Horizontal hydraulic gradient	0.02	0.08	0.02
Total groundwater travel time (yr)	10197	3781	6069
Discharge** (ft^3/yr)	2.7×10^7	1.1×10^7	3.6×10^7
Maximum release ratio***	1.2	3.9	1.5

*R = retardation factor
**annual recharge of regional ground water system is approximately 5×10^8 ft^3/yr
***maximum during 50,000 year period

6.3 Scenario 5: - Effects of changes in the water table

In scenario 5, the water table has risen 300 feet during a pluvial period and occurs in the densely welded tuff of layer H. Radionuclides migrate from the depository to this layer under the influence of the vertical hydraulic gradient (Figure 9). The zeolitized tuff of layer G is not a barrier to horizontal radionuclide migration in this scenario. In this calculation we have assumed that no retardation occurs in layer H. Ground water and dissolved radionuclides are pumped from the aquifer from a well located one mile from the depository. In all other respects, this scenario is equivalent to scenario 1.

Scenario 5B (Figure 10) differs from scenario 5 by the inclusion of matrix diffusion in calculations of radionuclide retardation in the moderately and densely welded layers A, C, E, F, and H. As in scenario 1B, retardation by matrix diffusion was considered only for ^{129}I, ^{99}Tc, and ^{14}C.

Results

The results of the calculations for scenario 5 are presented in Figures 11A-11E and in Table 9. It can be seen that the lack of retardation in the horizontal transport leg has resulted in discharges that are much larger than those calculated for scenario 1. Violation of the EPA Release limit results from discharges of ^{236}U, ^{233}U, ^{235}U, ^{238}U, ^{234}U, ^{228}Ra, ^{237}Np, ^{99}Tc, and ^{14}C. In the first 10,000 year period, discharge is entirely due to releases of ^{99}Tc and ^{14}C.

After 30,000 years, releases of other radionuclides comprise the major part of the discharge.

Results from scenario 5B are summarized in Figures 11A-11E and in Table 9. Matrix diffusion decreases the discharges of ^{99}Tc and ^{14}C to levels below the EPA release limit during the first 10,000 years. After 20,000 years, the release of ^{236}U, ^{228}Ra, ^{237}Np, ^{233}U, ^{229}Th, ^{238}U, ^{234}U, ^{210}Pb, ^{235}U and ^{227}Ac exceed the EPA Standard.

The properties of the vectors which violate the EPA Standard in scenario 5B are described in Table 10. The large radionuclide releases associated with vectors 3, 24, and 51 are due to their large groundwater discharge and short travel times. In vectors 72 and 85, the high horizontal darcy velocity is indicative of the short travel time associated with the horizontal legs

SCENARIO 5

1 mile well; moderate = fractured; thermal buoyancy; pluvial

LEG	LAYERS	WELDING - RETARDATION	LENGTH (ft)	
1	A	dense - no retardation	200	v
2	B	nonwelded - porous - zeolites	300	v
3	C	dense - no retardation	250	v
4	D	non-welded - porous - zeolites	150	v
5	E	moderate - no retardation	180	v
6	F	moderate - no retardation	270	v
7	G	nonwelded - porous - zeolites	475	v
8	H	dense - no retardation	5280	h

FLOW PATH
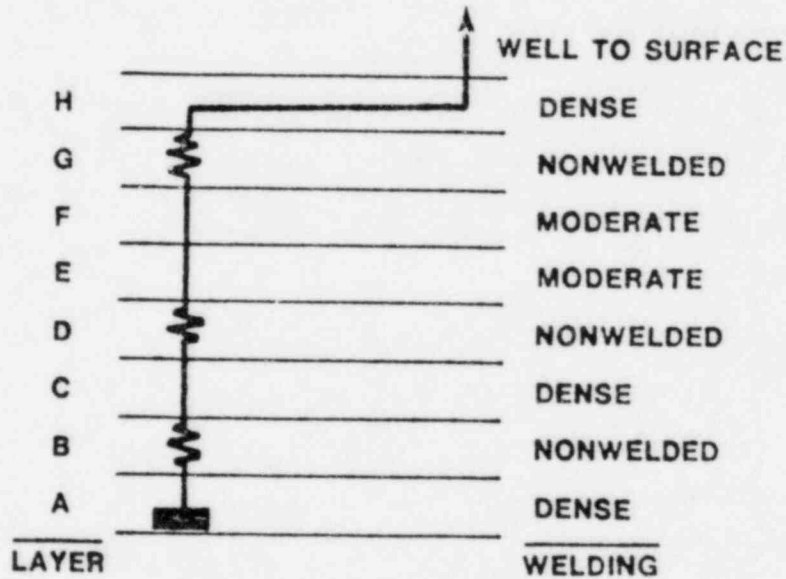
Figure 9

1 mile well; matrix diffusion; thermal buoyancy; pluvial

LEG	LAYERS	WELDING - RETARDATION	LENGTH (ft)	
1	A	dense - matrix diffusion	200	v
2	B	nonwelded - porous - zeolites	300	v
3	C	dense - matrix diffusion	250	v
4	D	non-welded - porous - zeolites	150	v
5	E	moderate - matrix diffusion	180	v
6	F	moderate - matrix diffusion	270	v
7	G	nonwelded - porous - zeolites	475	v
8	H	dense - matrix diffusion	5280	h

FLOW PATH

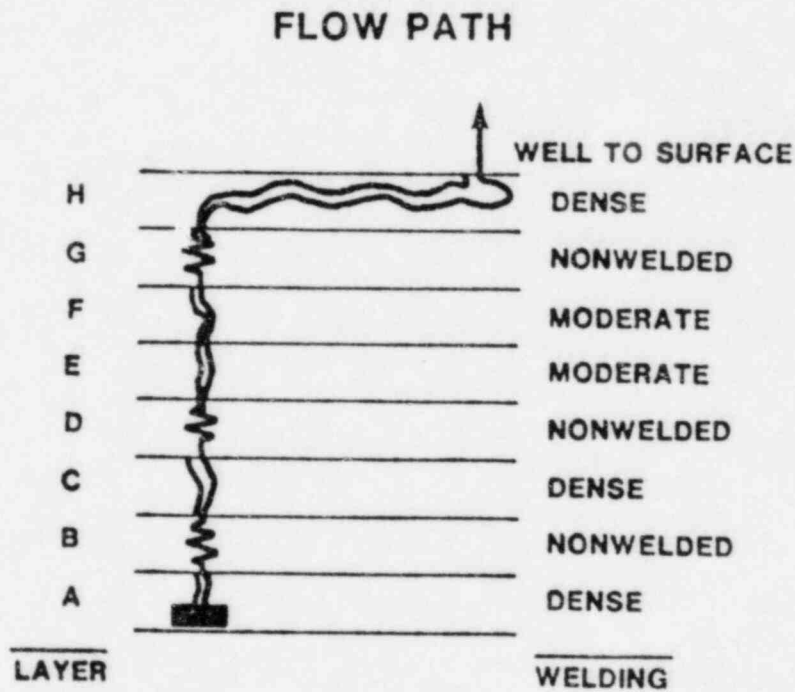
Figure 10

Table 9

NUMBER OF VIOLATING VECTORS, MAXIMUM OF RELEASE RATIOS AND SUM OF RELEASE RATIOS
OVER ALL VECTORS FOR EACH 10,000 YEAR PERIOD

Scenario	0-10,000yr	10,000-20,000yr	20,000-30,000yr	30,000-40,000yr	40,000-50,000yr
5	3*	6	11	14	16
	7.9**	6.2	20.9	43.7	54.0
	13.4***	29.6	54.2	102.1	178.8
5B	0	1	3	4	4
	0.90	2.1	19.3	42.1	53.4
	1.1	5.9	28.8	75.9	153.0
6	0	1	1	4	3
	0.1	1.5	1.6	4.4	2.2
	0.1	2.5	3.7	12.5	7.6
2	11	14	19	20	19
	207	85	87	57	55
	667	392	461	424	434
2B	8	10	16	17	19
	22	24	21	20	21
	62	114	116	123	130

*   number of violating vectors
**   maximum release ratio
*** sum of release ratios

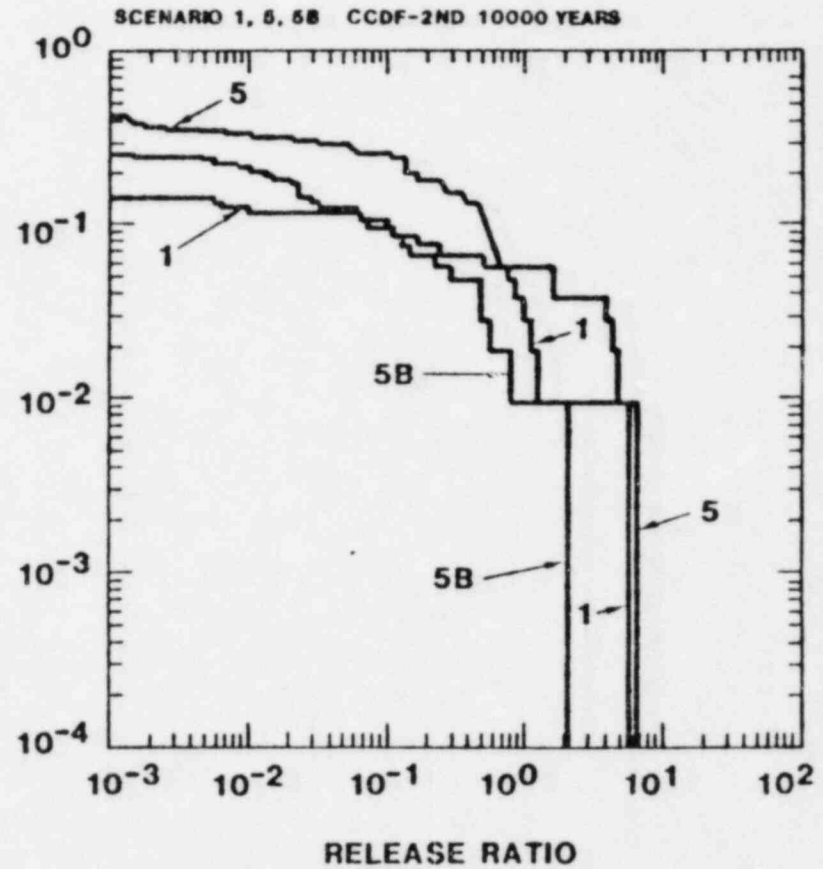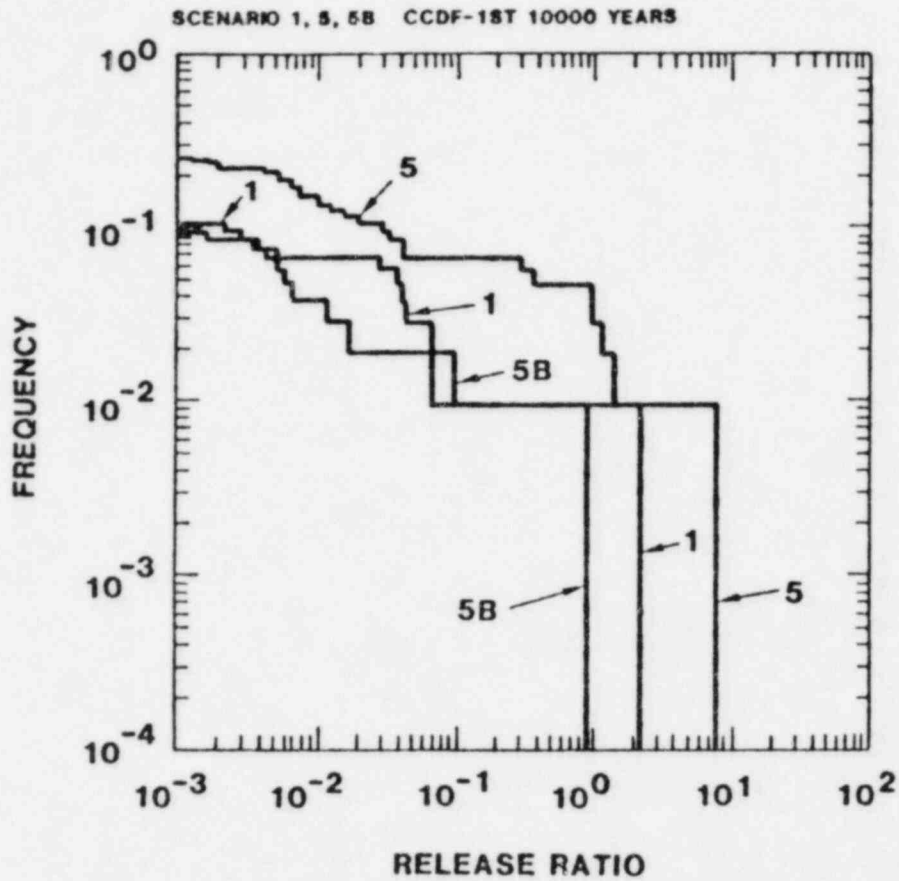-37-

Figure 11a.   Figure 11b.

Figure 11.   Complementary Cumulative Distribution Functions for Scenarios 1, 5 and 5B:
              Effects of Changes in the Water Table on Discharge.

              1 = base case; 5 = water table rise; 5B = water table rise with matrix
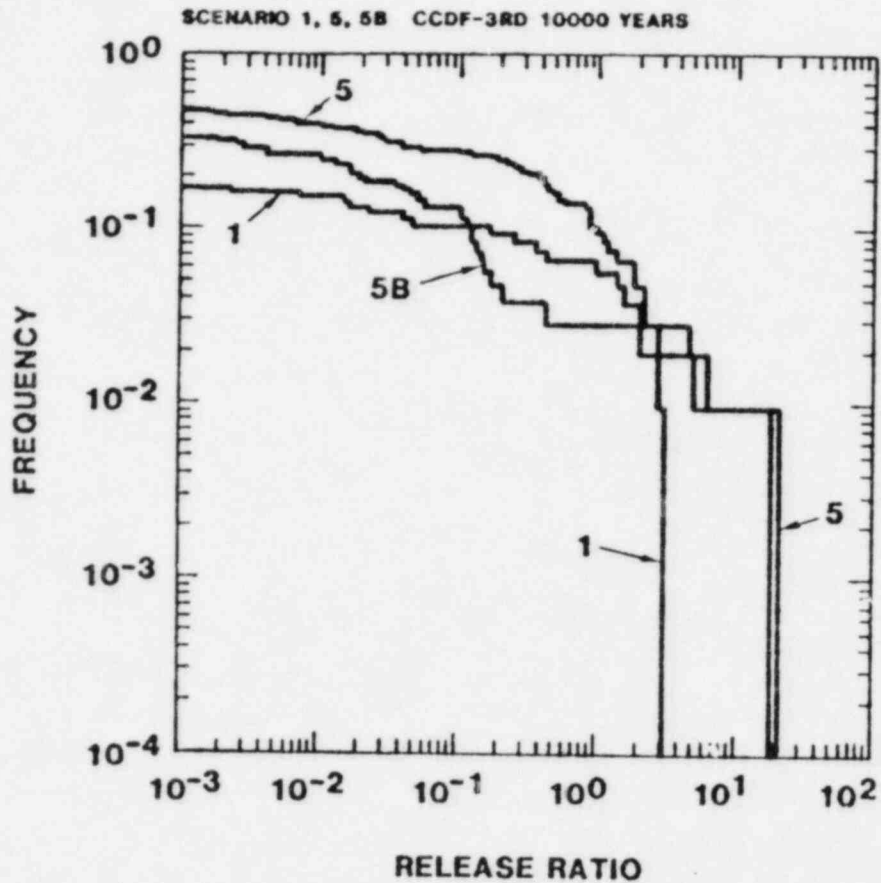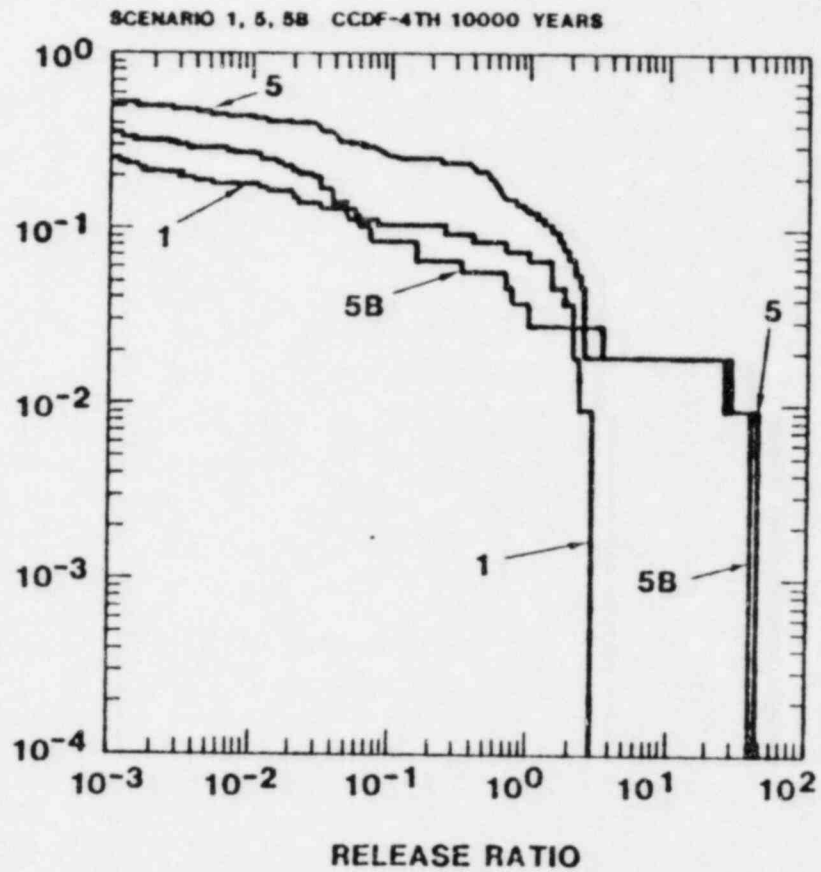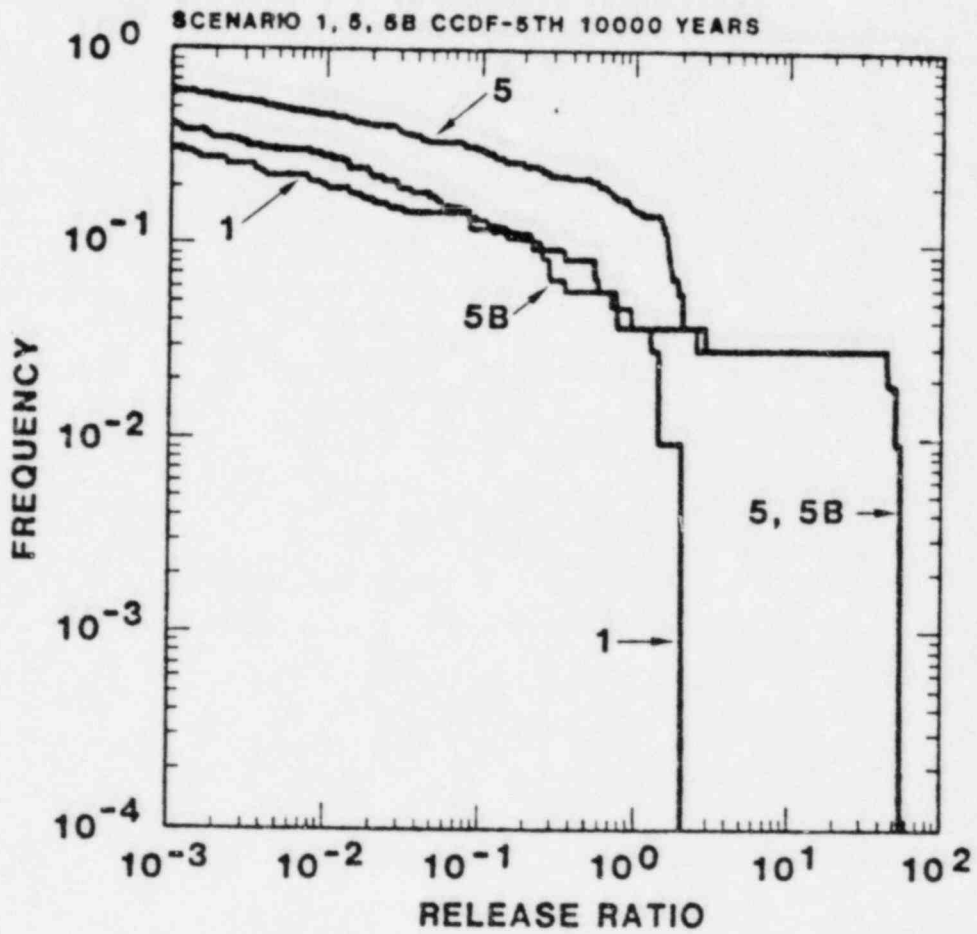   diffusion.

SCENARIO 1, 5, 5B   CCDF-3RD 10000 YEARS

SCENARIO 1, 5, 5B   CCDF-4TH 10000 YEARS

FREQUENCY

-39-

5

1

5B

1

5

RELEASE RATIO

Figure 11.c

5

1

5B

5

1

5B

RELEASE RATIO

Figure 11.d

Figure 11.e

Table 10

PROPERTIES OF VECTORS WHICH VIOLATE EPA STANDARD
IN SCENARIO 5B

VECTOR	3	24	51	72	85
PARAMETER					
Maximum R for U	32	27	23	47	35
Maximum R for Np	41	37	39	52	68
Maximum R for Tc	10827	20063	26659	13866	14888
Average vertical darcy velocity (ft/yr)	0.3	0.16	0.43	0.04	0.07
Vertical gradient	0.04	0.03	0.03	0.03	0.04
Average horizontal darcy velocity (ft/yr)	0.03	0.002	2×10^{-4}	1.5	169
Horizontal gradient	0.02	0.08	0.02	0.02	0.03
Total groundwater travel time (yr)	1024	2585	2203	7877	4939
Discharge (ft^3/yr)	2.7×10^7	1.4×10^7	3.8×10^7	3.5×10^6	6.1×10^7
Maximum release ratios					
U234	16	26	19	0	0
Np237	8.7	7×10^{-5}	12	0	0
Tc99	0	0	0	2.6	3.5
TOTAL	44.4	48.7	53.4	2.6	3.5

(0.03-0.6yr). Although the retardation factors for Tc in leg 3 are high for these vectors (5076 and 2569 respectively), the high darcy velocity indicates that this leg is not a barrier to migration of this radionuclide.

6.4 Scenario 6 - Accessible environment at eight miles

At the hypothetical repository site, the water table passes from the nonwelded zeolitized aquitard (layer G) into the overlying densely welded aquifer (layer H) at a distance of approximately two miles from the depository. In scenario 6, we have postulated that a well eight miles from the depository withdraws ground water and radionuclides from this aquifer. This scenario differs from scenario 1 by the additional one mile transport in the nonwelded unit and by six miles of transport in the densely welded tuff layer. No retardation occurs in the densely welded layer.

Results

The results of the calculation are presented in Figures 13A-13E and in Table 9. It can be seen that the additional seven miles of travel through layers G and H reduce the discharge during the first 10,000 years to levels below the EPA release limit. Discharges of the unretarded radionuclides ^{99}Tc and ^{14}C in vectors 12, 76, 77, and 105, however, exceed the EPA limit after 10,000 years. Due to time constraints, the effect of matrix diffusion on discharge was not calculated for the flow path of scenario 6. It was shown previously in scenario 1B that matrix diffusion in 900 feet of welded tuff decreased the discharge of ^{99}Tc and ^{14}C for the above vectors below the EPA Standard. It can be assumed, therefore, that matrix diffusion would eliminate all violations of the EPA Standard for a flow path similar to scenario 6.

8 mile well; moderate = fractured; thermal buoyancy; no pluvial

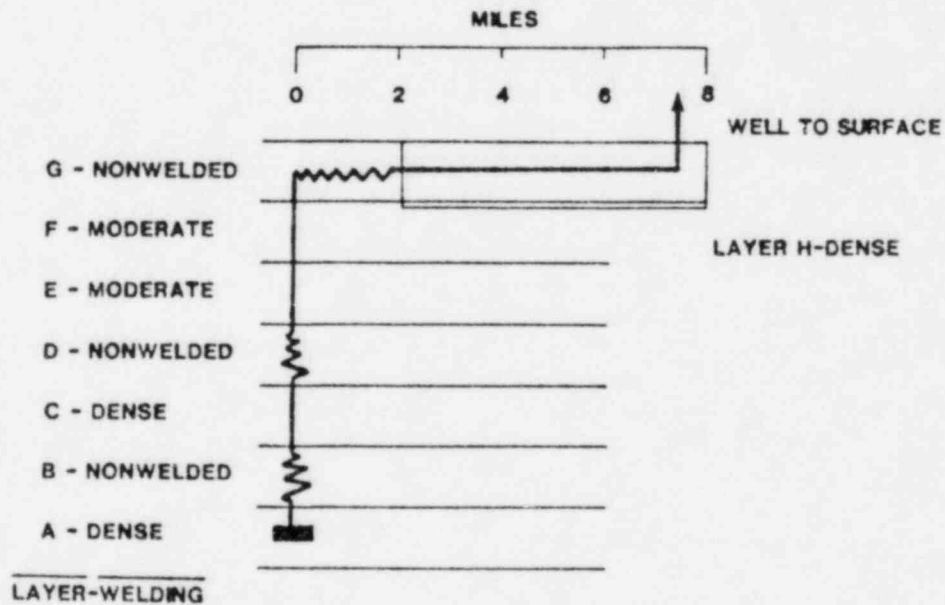| LEG	LAYERS	WELDING - RETARDATION	LENGTH (ft)	
1	A	dense - no retardation	200	v
2	B	nonwelded - porous - zeolites	300	v
3	C	dense - no retardation	250	v
4	D	non-welded - porous - zeolites	150	v
5	E	moderate - no retardation	180	v
6	F	moderate - no retardation	270	v
7	G	nonwelded - porous - zeolites	11000	h
8	H	dense - no retardation	31000	h

FLOW PATH

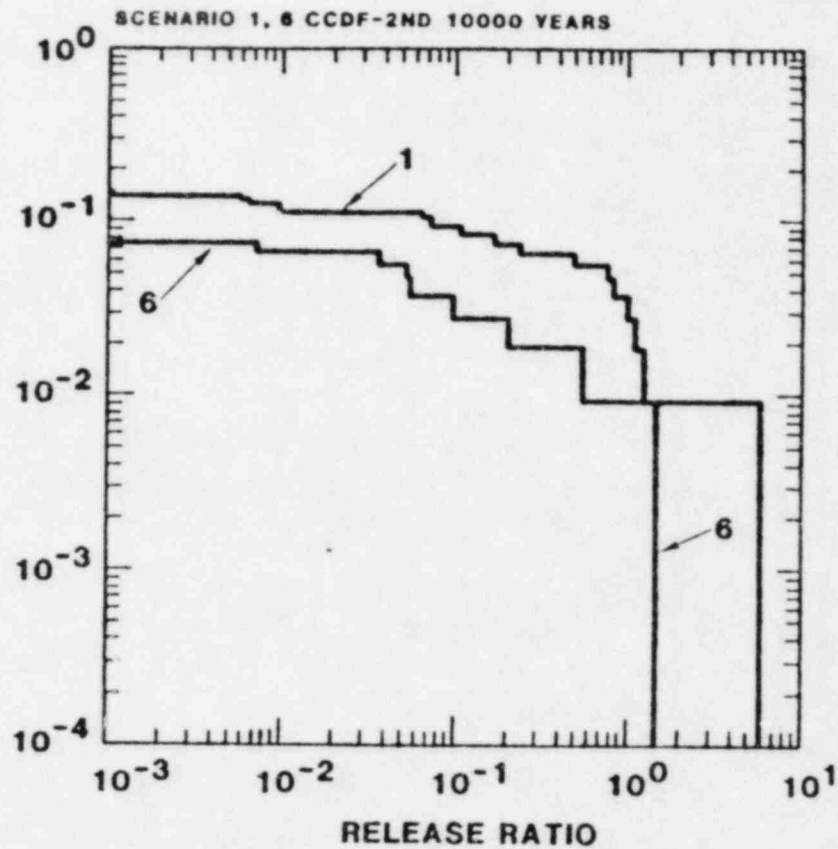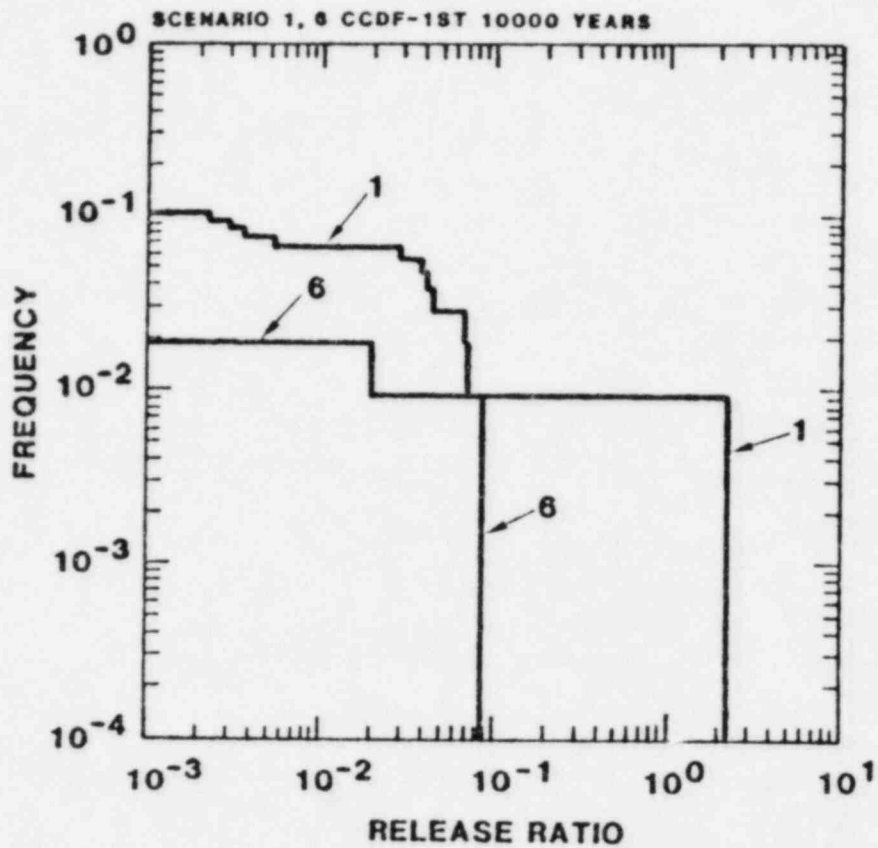Figure 12

-43-

Figure 13.a

Figure 13.b

Figure 13.   Complementary Cumulative Distribution Functions for Scenarios 1 and 6:
            Accessible environment at eight miles.

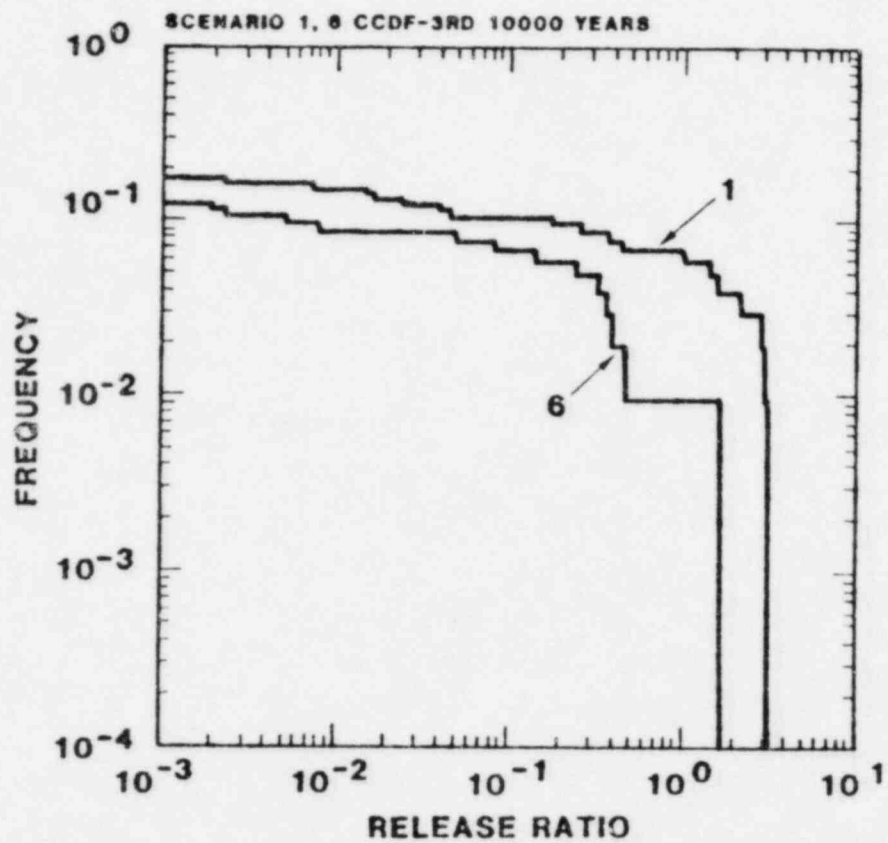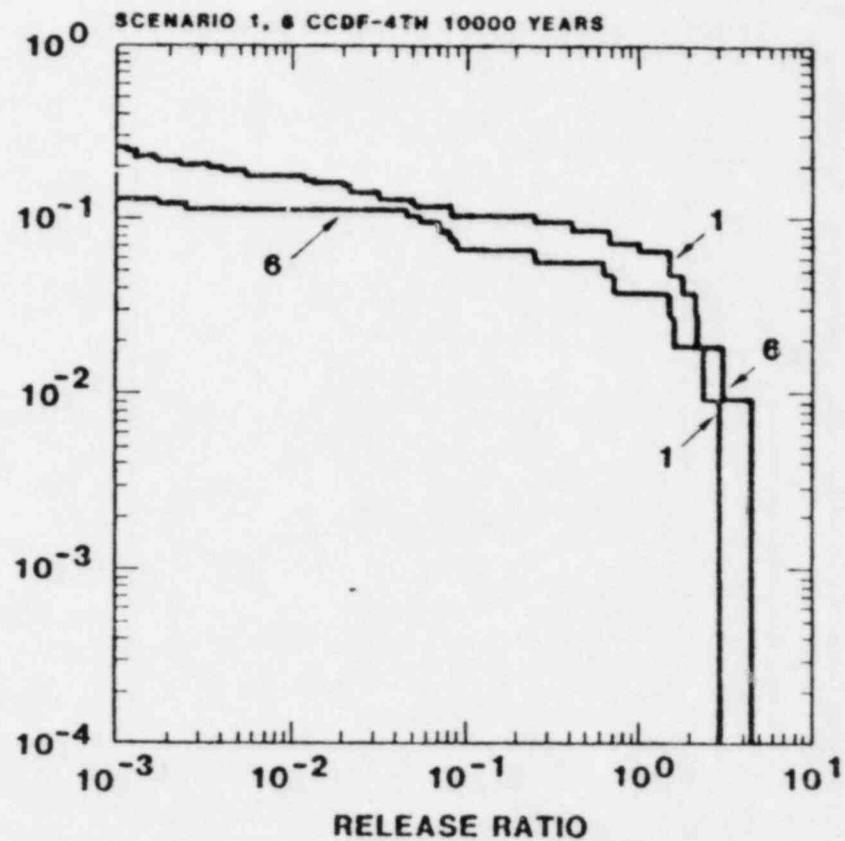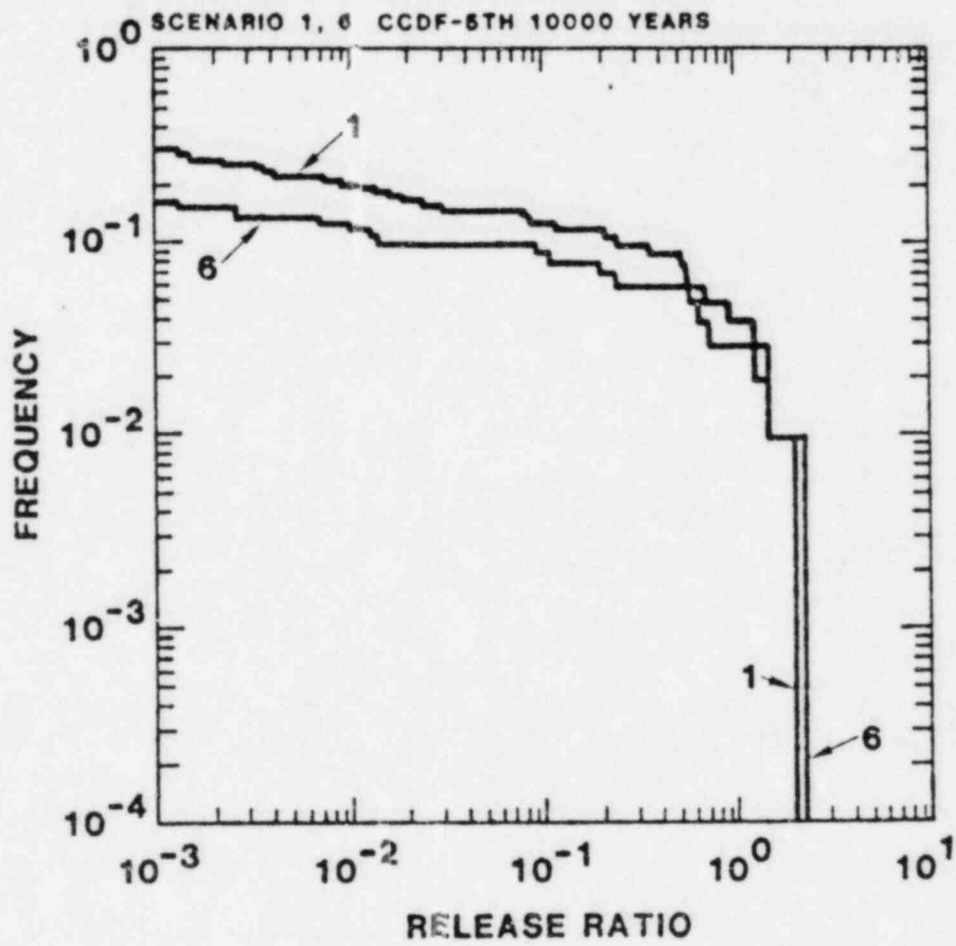   1 = base case; 6 = 8 miles

-44-

Figure 13.c

Figure 13.d

Figure 13.e

6.5 Scenarios 2 and 2B - Importance of solubility limits to
      discharge

We consider scenario 2 (Figure 14) our "worst case" scenario.
The source term is entirely leach-limited; the solubility
limits of radionuclide are not specified. Ground water
migrates laterally from the depository. Due to the block
faulting and dip of the tuff units in the repository site, the
lateral fluid flow path cuts across several stratigraphic
layers. At a distance of one mile from the depository, water
and radionuclides are pumped by a well that extends to a depth
of 3,000 feet. Technitium, ^{129}I and ^{14}C are retarded by
matrix diffusion in the densely welded layers A and C. Layer B
is highly sorbent zeolitic tuff which retards the movement of
the other isotopes. This scenario has a shorter path length
and thinner sequence of zeolitized tuff than the other sce-
narios.

Scenario 2B differs from scenario 2 only in the calculation of
the source term. We have used the mixing-cell option at
NWFT/DVM for this scenario (17,23). For each time step, the
mass of a radionuclide that is assumed leached from the waste
form is compared to the maximum amount that is consistent with
a user-specified solubility limit. The solubility limits are
listed in Table 5 and are discussed in detail in section 4.3
and in Appendix B. The smaller of these two amounts of radio-
nuclide is transported in that time step.

Results

Results of calculations for scenarios 2 and 2B are summarized
in Figures 15A-15E and in Table 9. Discharges in scenario 2
are the highest calculated in this study and lead to large vio-
lations of the EPA Standard. During the first 10,000 years,
releases of ^{234}U, ^{237}Np, ^{238}U and ^{236}U account for 94
percent of the sum of the EPA release ratios. During the fifth
10,000 year interval they continue to dominate discharge and
account for 85 percent of the violation of the EPA Standard.
The importance of solubility limits in controlling discharge in
scenario 2B can be seen in the figures and table. The sum of
the release ratios for all uranium species is reduced by an
order of magnitude and Np discharge is decreased by a factor of
30 for the first 10,000 year interval. Discharge of these
radionuclides, however, still are in excess of the EPA stan-
dard. The solubilities that were assumed for uranium and
neptunium were based on experimental studies under oxic condi-
tions. They are upper bounds for the solubilities; under
reducing conditions the solubilities of U and Np are 8 and 3
order of magnitudes lower respectively. We feel that the

SCENARIOS 2 and 2B

1 mile borehole; matrix diffusion; no thermal buoyancy or pluvial

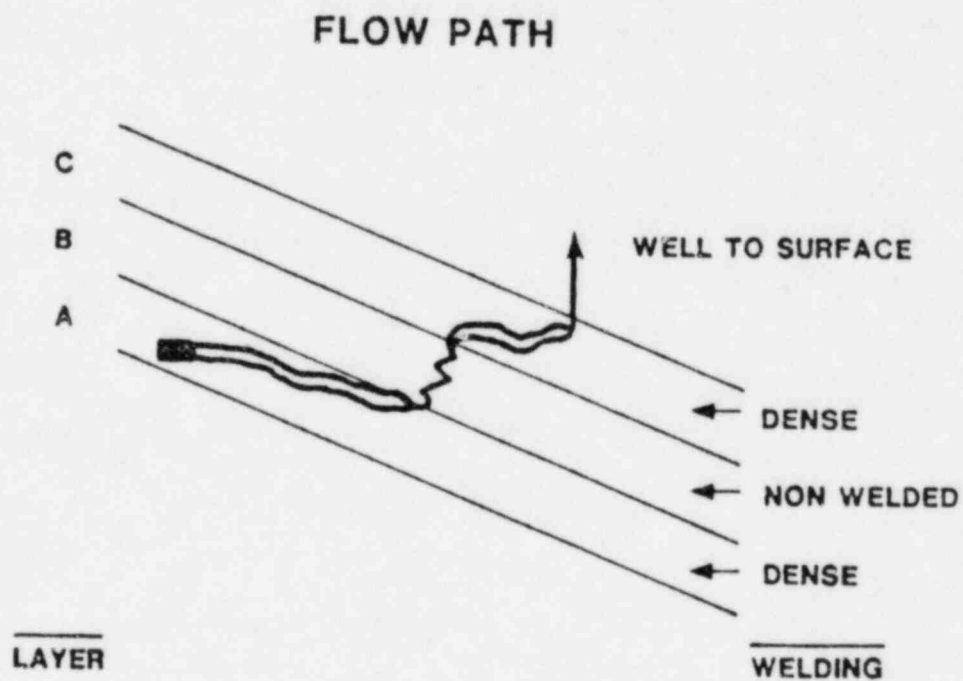| LEG	LAYERS	WELDING - RETARDATION	LENGTH (ft)	
1	A	dense - matrix diffusion	2600	h
2	B	nonwelded - zeolitized	300	v
3	C	dense - matrix diffusion	2600	h

FLOW PATH
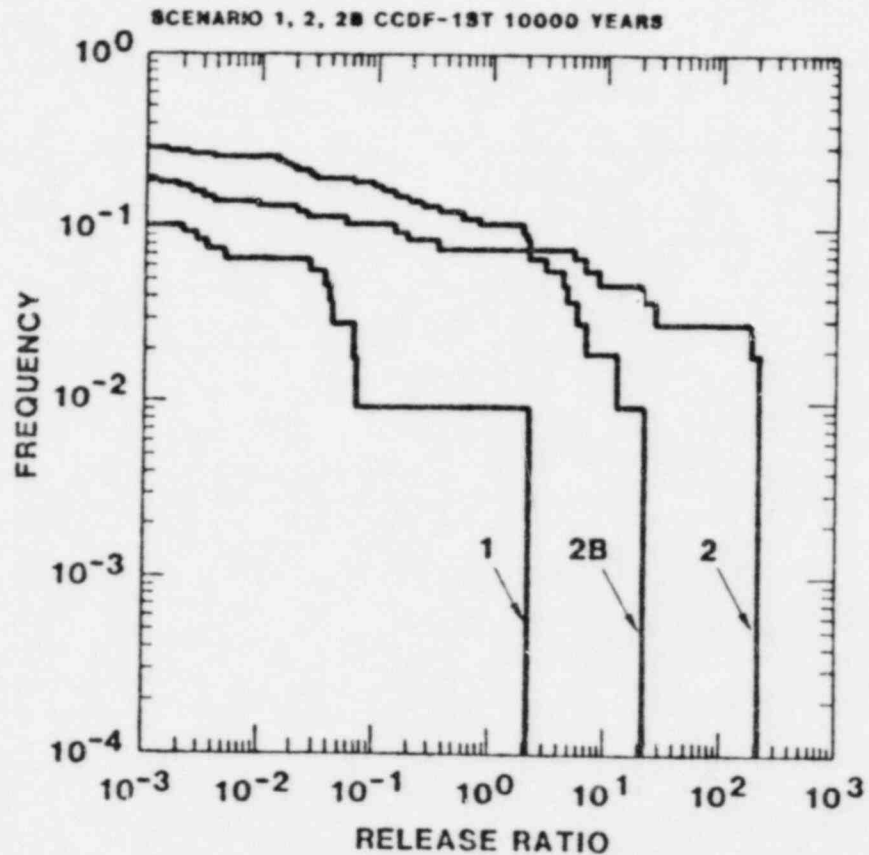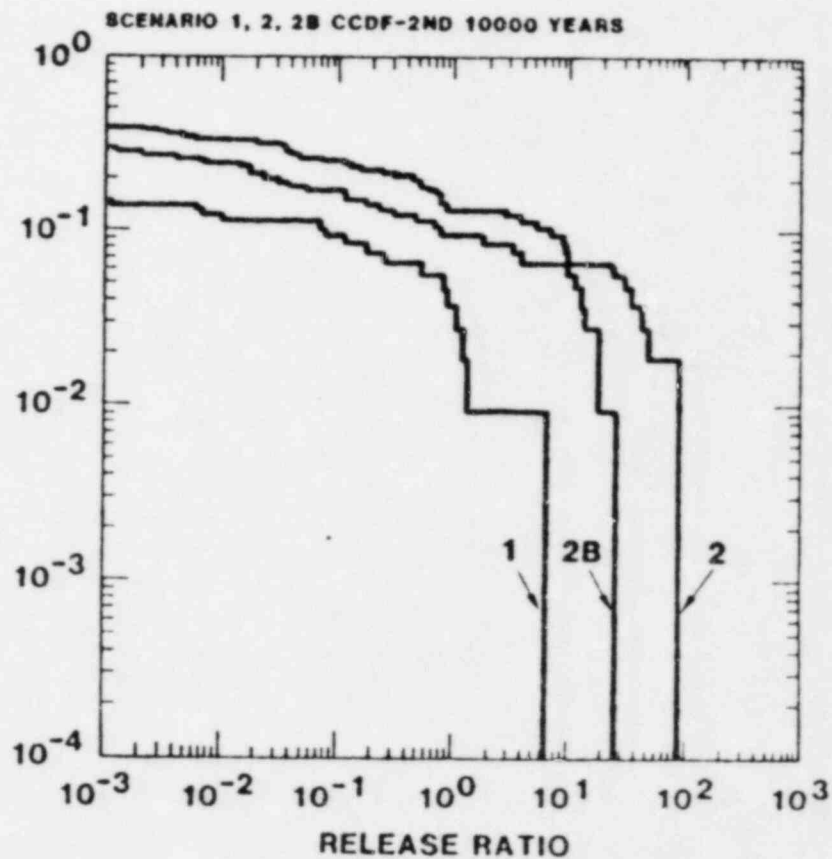

Figure 14

Figure 15.a

Figure 15.b

Figure 15.   Cumulative Complementary Distribution Functions for Scenarios 1, 2 and 2B:
            Importance of Solubility Limits to Discharge.

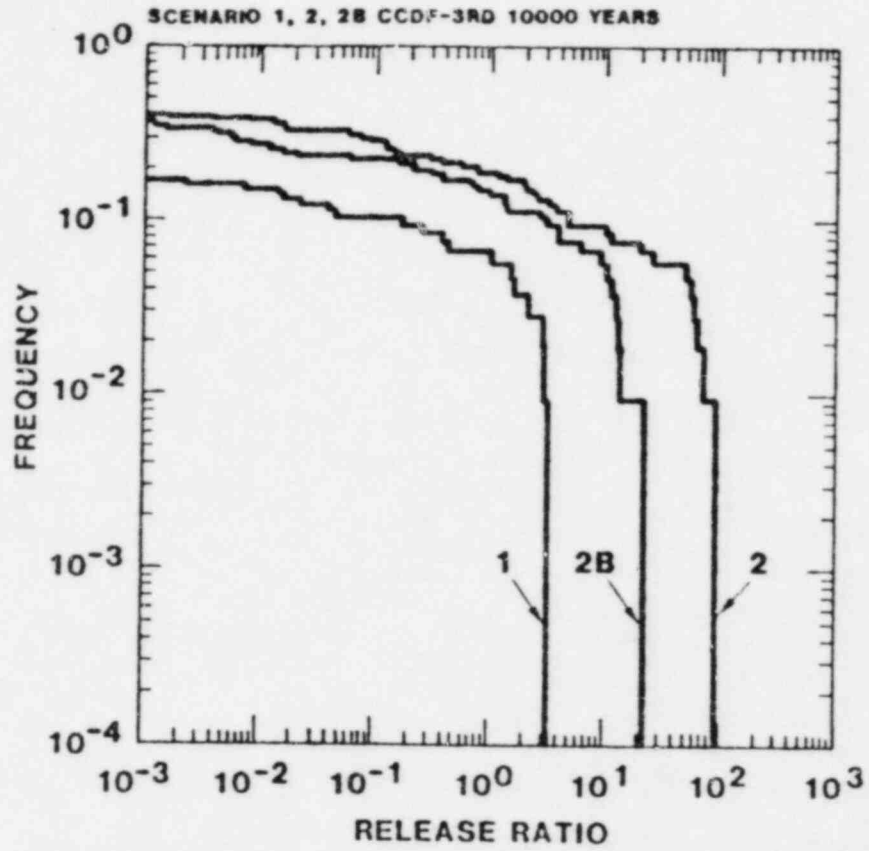   1 = base case; 2 = leach limited; 2B = solubility-limited
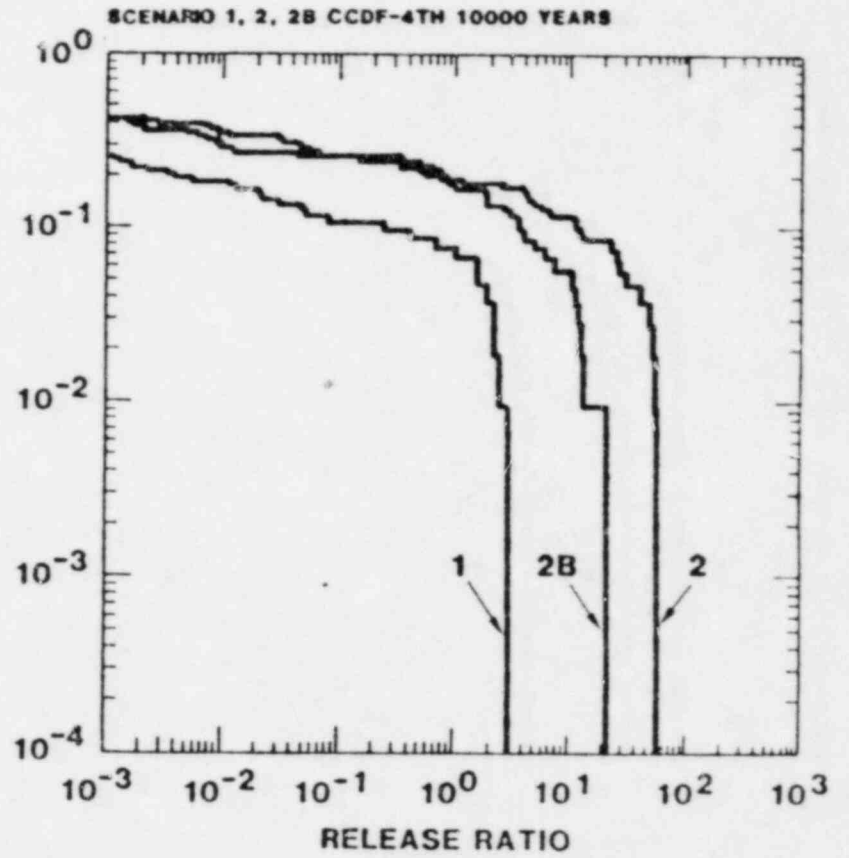
Figure 15.c
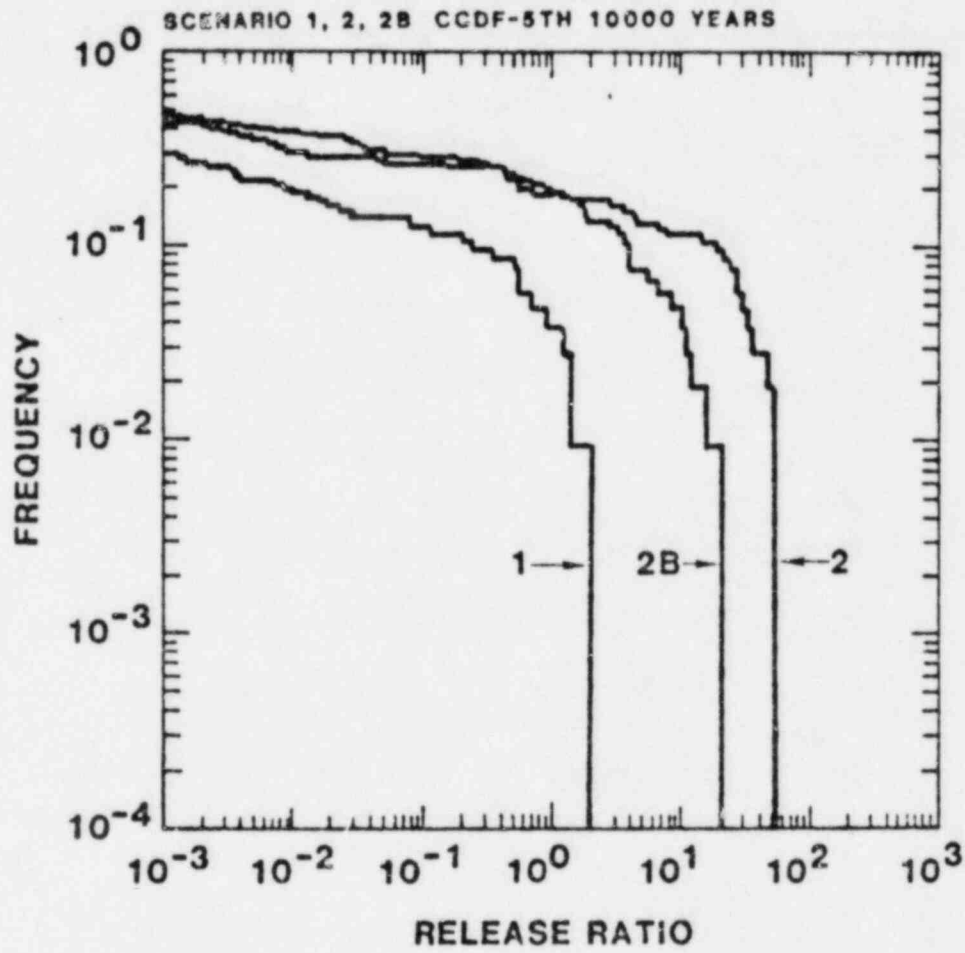
Figure 15.d

SCENARIO 1, 2, 2B CCDF-5TH 10000 YEARS

Figure 15.e

transport of radionuclides along the flow path described in scenarios 2 and 2B is less likely than transport as described in the other scenarios. The calculated violations of the EPA Standard, therefore, should not be interpreted as an indication that releases from a repository in tuff are likely.

7. CONCLUSIONS AND RECOMMENDATIONS

Estimates of potential radionuclide releases from HLW storage facilities in geologic formations are an integral part of the technical basis for the regulation of nuclear waste disposal. At present, the available data is insufficient to accurately model any real repository sites. Large uncertainties exist in the characterization of the solubilities and sorption of radionuclides, in the description of the regional and local hydrogeology and in the mathematical treatment of containment transport in the presence of fracture flow and matrix diffusion. We feel, however, that it is possible to place realistic upper limits on radionuclide discharge for a generic hypothetical tuff repository. We have also attempted to assess the importance of the variation of several variables and model assumptions to the calculations of radionuclide release from a repository in the saturated zone of a volcanic tuff site.

Our calculations suggest the following conclusions for the hypothetical tuff repository described in this paper:

1)   Sorption of radionuclides by several thousand feet of zeolitized tuff may be a sufficient barrier to migration of actinides even in the absence of solubility constraints.

2)   All violations of the EPA Draft Standard in the "base case" are due to discharge of ^{99}Tc and ^{14}C. Retardation due to matrix diffusion, however, could eliminate discharge of the nuclides for realistic groundwater flow rates.

3)   If the radionuclides do not flow through thick sequences of zeolitized tuff, discharges of U and Np under oxidizing conditions may be much larger than the EPA limits. Under reducing conditions, however, the low solubilities of these elements may reduce discharges of these elements to levels below the EPA limit.

We feel that the following topics merit further investigation by the NRC:

1)   Detailed calculations of limiting solubilities of uranium, neptunim and radium under geochemical conditions expected at the tuff site.

2)   Calculations of the potential retardation of actinides due to matrix diffusion in welded tuff.

3)   Calculations of the sensitivity of radionuclide discharges on assumptions about radionuclide speciation.

4)   A study of the frequency of oil and water drilling and mineral exploration in area like Yucca Mountain. All of the scenarios examined in this involve human intrusion. A study of the probability of such activities in areas like Yucca Mountain would yield valuable insights about the safety of such a repository site.

APPENDIX A

HYDROGEOLOGICAL MODEL OF THE HYPOTHETICAL TUFF REPOSITORY SITE AND ITS RELATIONSHIP TO DATA FROM THE NEVADA TEST SITE

A major objective in the program of simplified repository analyses performed at Sandia is the definition of a hypothetical site which exhibits hydrogeological characteristics which might be found at real potential repository sites. We have defined our reference tuff site to be consistent with available hydrogeologic data from the Nevada Test Site. Where certain data are not available from the real site, we have postulated properties that are physically reasonable for the reference site. We have not attempted to accurately represent the Nevada Test Site in our analyses; instead we have modelled a hypothetical site which is internally self-consistent.

A.1 Physical properties of welded tuff

The tuff units at the reference tuff repository are described as densely welded, moderately welded or non-welded. Densely welded tuff units are highly fractured; the blocks between fractures have low interstitial matrix porosity. Non-welded tuff units have few fractures but have a high matrix porosity. This dual porosity of the rock must be considered when modelling fluid flow. We have used data from the UE25a-1 drill core log to obtain reasonable values of fracture density, aperture width and orientation in the tuff units [1,2]. The maximum, minimum and median of the range of values of these parameters for different tuff lithologies are shown in Table A-1.

We have represented the fracture system as two sets of perpendicular vertical fractures. Values of horizontal fracture porosity (ϵ_h) here calculated by

$$\epsilon_h = N_a b \,/\, \sin(90° - \theta)$$

where N_a is the observed fracture density in the core, θ is an estimate of the average inclination of the fractures from the horizontal plane, and b is the fractures aperture width observed under a petrographic microscope. Horizontal hydraulic conductivity for a parallel array of planar fractures is given [24] by:

$$K_H = \left(\frac{\rho g}{\mu}\right) \left(\frac{N_a b^3}{2 \sin 90 - \theta}\right)$$

where:

ρ = density of water = 1.0 gm/cm^3
g = 9.81x10^4 cm^2 sec^{-1}
μ = viscosity of water = 1.0 centipoise

In our joint system, fluid flowing in the horizontal direction will effectively encounter only one set of fractures. Fluid flowing in the vertical direction will encounter both sets of fractures. For this reason, values of hydraulic conductivity and fracture porosity in the vertical direction are twice the horizontal values.

The hydraulic conductivity is very sensitive to changes in fracture aperture. In welded zones, the majority of fractures were 5-20 microns wide; the maximum observed width was 150 microns. Fractures in non-welded zones were generally filled with secondary minerals. For these units, aperture widths of 0-5 microns are probably realistic and were used to estimate the hydraulic properties in Table A-1. Results of calculations using a 150 microns aperture width are also shown in the table. Ranges of values of total porosity are presented and are taken from data in References 4 and 25.
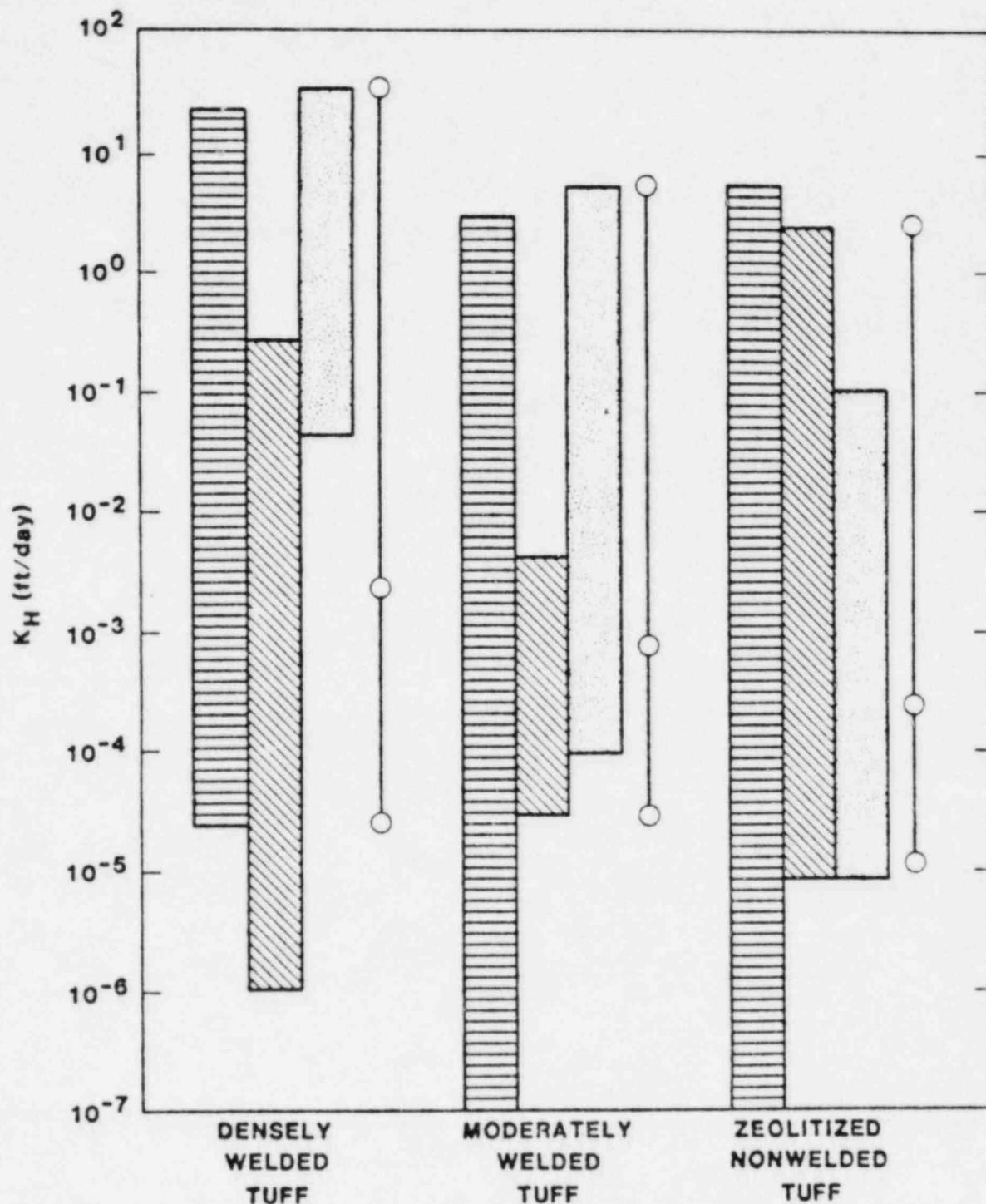
In Figure A-1, the ranges of values of matrix hydraulic conductivity of unfractured cores of tuff measured in the laboratory are compared to the values calculated from fracture properties. The values are based on data compiled in References 4, 22, and 25. Values of the bulk hydraulic conductivity as measured by actual pump tests at the Nevada Test Site are also shown. Data obtained in these tests reflect contributions from fluid flow in both the fractures and in the rock matrix between joints. It can be seen that flow in fractures may dominate the bulk hydraulic conductivity of densely welded tuffs whereas fluid flow in the porous rock matrix dominates the properties of non-welded units. Both fracture flow and porous flow are important for moderately welded tuffs. The insights gained from Figure A-1 were used to estimate reasonable ranges for effective porosity and hydraulic conductivity for the Latin Hypercube Sample. The data ranges and the shape of their distributions are tabulated in Table 2 of the main text. The shapes of the frequency distributions were estimated by comparing the median values to the upper and lower limits of the data ranges of the different types of hydraulic conductivity and porosity.

A.2 Vertical Hydraulic Gradient

There are insufficient data in the open literature at present to estimate vertical hydraulic gradients at the Nevada Test

Table A-1

PROPERTIES OF FRACTURED TUFF

	Densely Welded Tuff	Moderately Welded Tuff	Non-Welded Tuff
Fracture Aperture - b (microns)			
min	5	5	0
median	12	12	5
max	150	150	5 (150)
Apparent Fracture Density - N_a (ft^{-1})			
min	0.2	0	0
median	1.2	0.4	0.1
max	4.8	0.8	0.3
Inclination of Fractures from Horizontal (θ)	42°	45°	80°
Horizontal Fracture Porosity - ϵ (%)			
min	4.4×10^{-4}	0	0
median	6.4×10^{-3}	2.2×10^{-3}	9.5×10^{-4}
max	0.32	0.06	2.8×10^{-3} (0.09)
Horizontal Fracture Hydraulic Conductivity (K_H)			
min	2.6×10^{-5}	0	0
median	2.1×10^{-3}	7.5×10^{-4}	5.5×10^{-5}
max	16.7	2.9	1.7×10^{-4} (4.5)
Total Porosity (%)	3-10	10-38	20-50

RANGES OF VALUES OF HYDRAULIC CONDUCTIVITY
DETERMINED BY DIFFERENT METHODS

Figure A-1

Site with an acceptable degree of certainty. In our reference
site, we have assumed that the vertical gradient in the vicin-
ity of the repository will be dominated by a thermal bouyancy
gradient related to heat generated by the decay of the radio-
active waste. The calculation of the thermal bouyancy gradient
is described below.

Consider a cylindrical volume of fluid with length L and
average temperature T immersed in a medium of average tempera-
ture T_0 (T T_0), (Figure D-1). The difference in tempera-
ture produces an upward force on the volume of fluid. The
velocity of the fluid in the cylindrical volume can be
described (26) by:

$$v \sim \alpha \Delta T K \qquad (A-1)$$

with

    v = Darcy velocity of fluid

    α = average coefficient of thermal
         expansion of fluid

    $\Delta T = T - T_0$

    K = hydraulic conductivity of medium
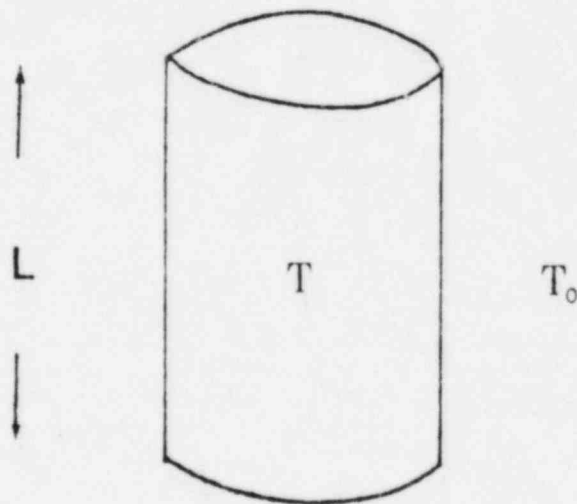
Figure (A-2)

Since Darcy velocity is equal to the product of hydraulic gra-
dient (I) and conductivity, the upward gradient is given by

$$I = \alpha \Delta T \qquad (A-2)$$

The temperature field around a repository in tuff for spent-fuel at 75 kW/Acre thermal loading has been calculated (3).
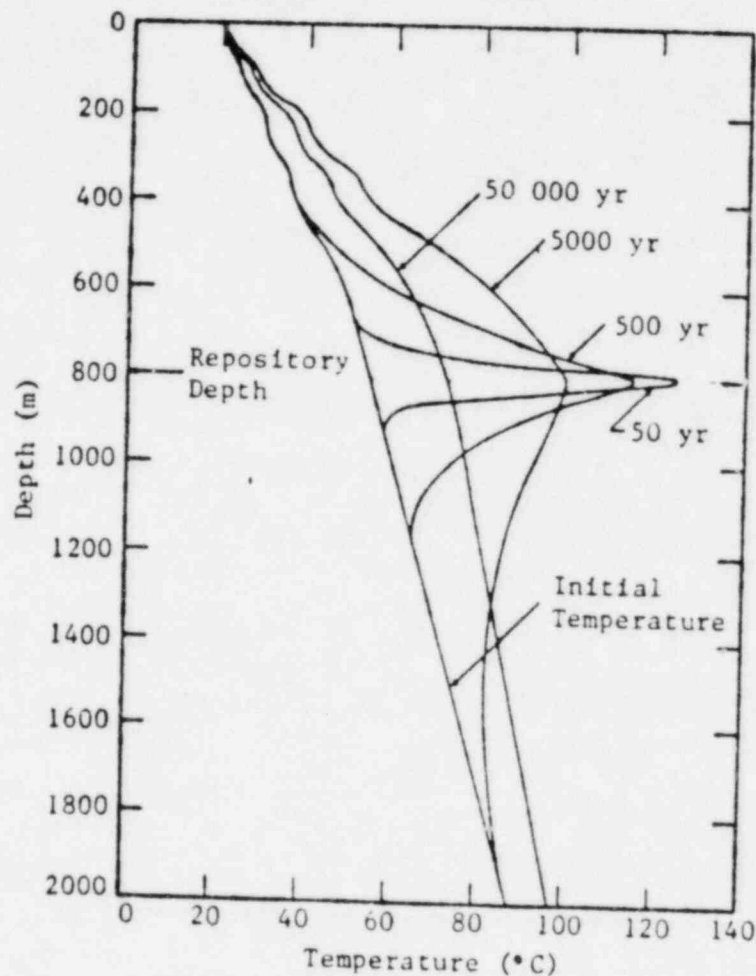
Figure (A-3) Far Field Temperature Profile Along the Vertical Centerline for GTL of 75 kW/Acre

Figure A-3 shows the temperature profile along the vertical centerline of the repository as a function of depth and time after closure. The "disturbed zone" is assumed to extend from the repository to 470 meters below surface where the water table lies. The average temperature of this disturbed zone is calculated by:

$$\overline{T} = \frac{1}{L} \int T \, dL$$

L is the distance from the repository to the water table and is equal to 330 meters. To is the average background temperature of the same zone as calculated from the natural geothermal field. The ambient temperature at the repository horizon is 50°C. Under these assumptions, the hydraulic gradients calculated are shown in Table A-2:

Table A-2

Time After Closure	$\bar{T}$ (°C)	T_0 (°C)	α (1/°C)	Gradient
500 y.	73°	50°	6.01×10^{-4}	1.4×10^{-2}
5,000 y.	85°	50°	6.68×10^{-4}	2.3×10^{-2}
50,000 y.	65.4°	50°	5.54×10^{-4}	8.5×10^{-3}

More recent field work indicates that the ambient rock temperature at the repository horizon will be 35°C (27). Table A-3 shows the calculated upward gradient when this temperature is assumed.

Table A-3

Time	$\bar{T}$ (°C)	T_0 (°C)	α (1/°C)	Gradient
500 y.	73°C	30°C	6.01×10^{-4}	2.6×10^{-2}
5,000 y.	85°C	30°C	6.68×10^{-4}	3.7×10^{-2}
50,000 y.	65.4°C	30°C	5.54×10^{-4}	1.9×10^{-2}

Thermal histories at 307 and 711 meters below the surface for a repository with a 100 kW/Acre thermal loading have been calculated and are presented in Figure A-4 (27). From these curves, it is apparent that the peak temperature occurs before 10,000 years after closure of the facility. The hydraulic gradient at 500 years for an average ambient temperature of 50° was selected as a lower bound for our calculations. The gradient at 5,000 years with the average ambient temperature of 30° was used as the upper bound for the vertical hydraulic gradient. A range of vertical hydraulic gradients of 1×10^{-2} to 4×10^{-2} was sampled by the Latin Hypercube Sample technique for the transport calculations.
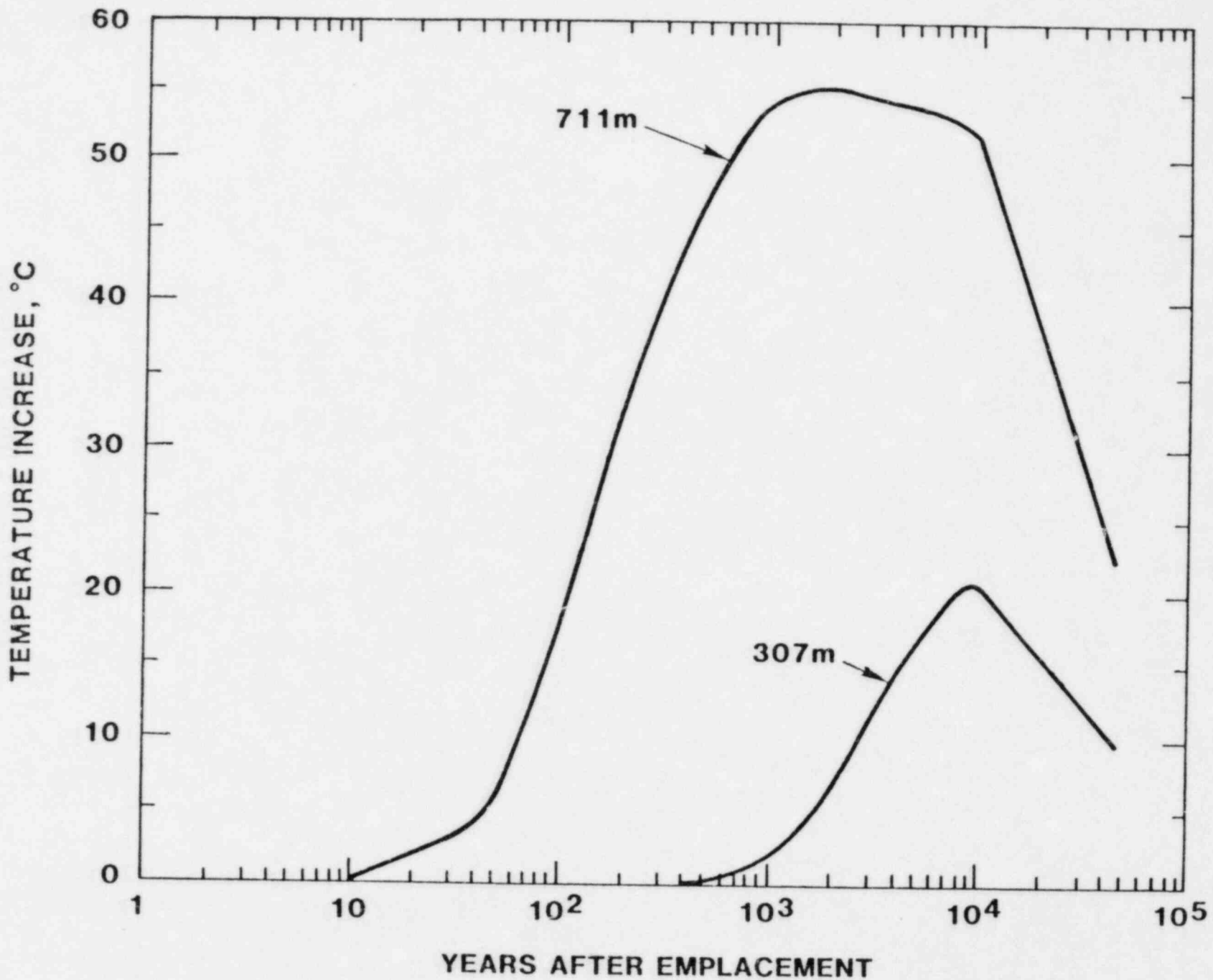
Figure A-4. Temperature increase histories at 307 and 711 meters below the surface of the earth for SF at 100 kW/acre.

The volume of annual recharge at the repository site places a
constraint on the maximum flow through the repository under the
influence of this thermal gradient. The maximum vertical dis-
charge calculated from the vectors sampled by the LHS technique
was 3.6×10^7 ft^3/yr (vector #51). This is approximately 7
percent of the volume of ground water moving through the
Pahute Mesa ground water system. The area of the repository
comprises less than 0.1 percent of the area of this flow sys-
tem. Although all of the recharge in this system is limited to
areas above 5000 feet elevation, this volume of groundwater
flow through the repository is probably unrealistically high.
As discussed in Section 6 (Table 7), nearly all of the vectors
whose radionuclides releases violated the EPA Standard in scen-
arios 1, 3, 4, 5, 6, 1B, and 5B were characterized by similarly
unrealistic flows. Most of the other vectors considered in
these calculations had ground water discharges at least an
order of magnitude smaller than vector #51.

A.3   Horizontal Hydraulic Gradient

We have considered two contributions to the horizontal
hydraulic gradient in our calculations. One component is the
regional gradient of the undisturbed site. Static water levels
from four wells near Yucca Mountain were used to estimate
ranges of the regional horizontal gradient. Three of the wells
have similar static water levels ($\sim$ 2400 ft) while the fourth
and only well which is actually on Yucca Mountain has an ano-
malously high head ($\sim$ 3400 ft) (22, 28). The range of regional
hydraulic gradients was set to span the highest and lowest
valued that could be calculated from these data. The LHS rou-
tine, therefore, sampled a range of 10^{-1} to 10^{-3}.

The second component to the horizontal gradient is a local
gradient related to the local rise in the water table above the
repository due to the thermal bouyancy effect described pre-
viously. We can place an upper bound on this rise in water
table (ΔZ) by assuming that the heated water in the cylinder
described in Figure A-2 is constrained to expand only in the
upward ($\hat{Z}$) direction. By applying Archimedes Principle, we
can show that the height of the heated cylinder can be related
to the height of a cylinder of water of equal weight at the
background temperature To. Since the height of the cylinder of
water at temperature To equals the distance from the repository
to the water table we can calculate ΔZ as follows:

-62-

$$w = \pi r^2 g \rho (L + \Delta Z) = \pi r^2 g \rho L \qquad \text{Archimedes Principle} \qquad \text{(A-3)}$$

$$\Delta Z = L(\rho/\overline{\rho} - 1) \qquad \text{(A-4)}$$

where

$\rho, \overline{\rho}$ = average density of water at To and T respectively
L = height of cylinder of water at temperature To
r = radius of cylinder of water
ΔZ = rise of water table
w = weight of water in both cylinders

If V equals the volume of the cylinder of water at temperature To, then

$$w = \rho V = \overline{\rho}(V + \Delta V) \qquad \text{(A-5)}$$

$$\Delta V = \alpha V \Delta T \qquad \text{(A-6)}$$

$$\overline{\rho} = w/V(1 + \alpha \Delta T) = \rho/(1 + \alpha \Delta T) \qquad \text{(A-7)}$$

where ΔT and ΔV refer to differences in temperature and volume between the two cylinders and α is the average coefficient of thermal expansion of the fluid. Substituting (A-7 into A-4) we obtain:

$$\Delta Z = L \alpha \Delta T \qquad \text{(A-8)}$$

We have shown that $\alpha \Delta T$ is equal to Iv, the vertical hydraulic gradient (equation A-2). We can therefore calculate ΔZ for each input vector in our calculations by using the value of Iv sampled by the LHS technique. The horizontal hydraulic gradient (I_H) used in our transport calculations is set equal to the sum of the regional gradient and the local gradient:

$$I_H = I_{HS} + I_V L/X \qquad \text{(A-9)}$$

where:

I_{HS} = value of regional horizontal hydraulic gradient sampled by the LHS

I_V = value of vertical gradient sampled by LHS

L = sum of vertical leg lengths in transport path

X = sum of horizontal leg lengths in transport path

APPENDIX B

GEOCHEMISTRY AND RADIONUCLIDE RETARDATION

B.1 - Geochemical environment of the hypothetical tuff site

The mineralogy of each rock unit at the hypothetical tuff site is described in Table 1. The mineralogy and chemical composition of a tuff unit depend in part upon its cooling history and degree of post-depositional alteration. Vitric tuffs are porous tuffs which are composed of pumice or fragments of glass shards which have undergone a moderate to slight degree of welding. Their chemical composition is simple; the sum SiO_2 + Al_2O_3 + K_2O + Na_2O is greater than 95 weight percent. Minor elements include Ca, Mg, Cl, F and transition metals. Alteration of the glass to clay is ubiquitous in minor amounts and locally may be nearly complete. Devitrified tuffs are chemically very similar to vitric tuffs but are quite different in their mineralogy and physical properties. They are composed primarily of fine-grained aggregates of sanadine and cristobalite. They may contain phenocrysts of amphiboles, clinopyroxene and feldspar as well as lithic clasts. Low temperature alteration of devitrified tuffs is not significant; access of ground water to the rocks is limited by the low interstitial porosity. Zeolitized tuffs are the products of low temperature alteration of non-welded volcanic ash. They are composed primarily of the zeolites clinoptilolite, mordenite, and analcime.

An average chemical composition of the ground water (6) is shown in Table B-1. The water is classified as a sodium-potassium-bicarbonate water by Winograd et. al. (4). Locally the composition of ground water is dependent upon lithology. Waters associated with vitric tuffs are highest in silica, sodium, calcium and magnesium whereas ground water in zeolitic tuffs is depleted in the bivalent cations (29). The pH of these waters ranges from near-neutral to slightly alkaline (7.2-8.5). The Eh of the groundwaters in the repository horizon is unknown. Dissolved oxygen contents from several shallow wells from the Nevada Test Site are fairly high (~ 5 ppm) (30). The concentrations of several redox indicators and the alteration features of the mafic minerals in several units indicate that oxidizing conditions prevailed at one time below the water table (9). Negative redox potentials and low levels of dissolved oxygen, however, have been measured in sections of a drill hole in the Crater Flat Tuff (31). These observations are consistent with measured values of sulfide in the ground-water and the occurrence of pyrite (FeS_2) in the rock matrix. The measurements are subject to a large amount of

TABLE B-1

ANALYSES OF WATERS FROM THE NEVADA TEST SITE (mg/l)

Well Species	J-13[1]	USW-H1[2]	USW-VH1[2]
Na^+	47.00	74.90	97.10
K^+	4.70	5.10	4.30
Ca^{+2}	13.00	7.20	10.30
Mg^{+2}	2.00	0.40	1.90
Ba^{+2}	0.20	0.01	0.04
Sr^{+2}	0.06	0.02	0.08
$HCO_3^- + CO_3^{-2}$	130.00		
Cl^-	7.70		
SO_4^{-2}	21.00		
NO_3^{-2}	5.60		
F^-	1.70		
SiO_2	61.00	11.00	53.40
pH	7.1-8.3	-	-
TDS	> 294.00		

[1] LA-7480-MS - reference 6
[2] LA-8847-PR - reference 8

uncertainty and must be confirmed by further investigations. In light of this uncertainty, we assumed that the ground waters at the hypothetical repository are oxidizing. The importance of redox to both the solubilities and Rd values for the radionuclides that were considered in our calculations will be discussed below.

B.2 Radionuclide Solubilities

As discussed in Section 4.3, we have attempted to estimate upper bounds for the radionuclide solubilities at the tuff repository. These limits were set after a limited review of available experimental data and theoretical calculations. Most of the redox-sensitive elements are least soluble under reducing conditions. In light of the uncertainty concerning the redox conditions at Yucca Mountain and in order to ensure that our calculated releases are conservative, we have used the estimated radionuclide solubilities for oxic conditions in our calculations.

The estimated solubility limit for each element is discussed below. In our calculations, a pH = 8 and a ground water composition similar to J-13 water (Table B-1) were assumed.

Pu: Experimental studies reviewed by Wood and Rai (15) suggest that Pu solubility is relatively insensitive to redox conditions. They suggested a value of 4×10^{-10} M from their data. A more conservative value of 10^{-3} M (2.4×10^{-4} gm/gm) was used in order to account for the possible dominance of a Pu-carbonate complex (31).

U: Uranium solubility could be very high if considerable CO_3^{2-} is present. However, the ground water composition at NTS (6,8) does not support this possibility. We have used the experimental data presented in (15) to set the U solubility limit at 2.4×10^{-5} gm/gm. Under reducing conditions the solubility would be approximately 8 orders of magnitude lower.

Th: The dominant species at Th is probably Th(OH)$_4$° at pH's above 5 (13,32,33). We used the reaction:

$$Th(OH)_4° \gtrless ThO_2(s) + 2H_2O$$

to estimate the solubility limit at 2.3×10^{-7} gm/gm at pH=8. The solubility is not sensitive to redox.

Ra: Radium is another element whose solubility is relatively insensitive to redox. Its solubility is controlled primarily by $RaSO_4(s)$ or $RaCO_3(s)$. The value from (16) is a very conservative upper bound for Ra solubility at the tuff site.

Cm: Few data are available to estimate Cm solubility in natural waters. In a 0.1M NaCl solution at pH=3, the Cm solubility was 10^{-11}M. The solubility decreases at lower pH (14). A conservative value of 10^{-10} M (2.5×10^{-11} gm/gm) was used in the calculations.

Am: Am solubility has been studied by Wood and Rai (15). They suggest that a value of 7×10^{-12} M is reasonable over a wide range of redox conditions. Complexing by Cl^-, SO_4^{2-}, or NO_3^{2-} will not be significant.

Np: Neptunium is least soluble under reducing conditions (10^{-10}M) (15). At an Eh = +0.26 and pH=7 the solubility of NpO_2 (c) is approximately 2.4×10^{-8} gm/gm.

Pb: PbCO$_3$ or PbSO$_4$ will limit the solubility of lead in an oxic tuff environment to less than 10^{-6} M. If any sulfide is present, PbS will precipitate and further decrease the solubility.

Pa: Little data are available for proactinium solubility in natural waters. We use the reactions:

$$Pa^{4+} + 4OH^- \rightleftharpoons Pa(OH)_4^\circ$$
$$PaO_2 + 2H_2O \rightleftharpoons Pa^{4+} \pm 4OH^-$$
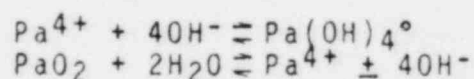
to set the solubility limit at 2.3×10^{-2} M.

Ac: We had no data to estimate the solubility of actinium; we therefore assumed that it had no solubility limit for in calculations.

Tc: Tc is least soluble under reducing conditions and precipitates as TcO$_2$. Under oxidizing conditions it is probably present as TcO$_4^-$ and is very soluble. We have assumed that it is not limiting solubility in our calculations (13, 16).

I, Cs: These elements probably have no limiting solubilities under repository conditions (13, 16).

Sn: We have assumed that these redox-insensitive reactions determine the solubility of tin (13, 16):

$$Sn^{4+} + 4H_2O = Sn(OH)_4^\circ + 4H^+: \quad \log K = -57$$
$$Sn(OH)_4(s) = Sn^{4+} + 4OH^-: \quad \log K = -0.87$$
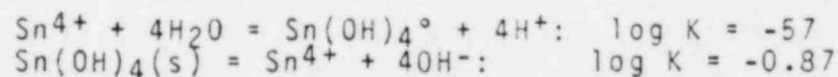
Sr: The solubility of Sr is probably set by strontianite SrCO$_3$ (13, 16). At pH=8, the reported 130 ppm of HCO$_3^-$ + CO$_3^{2-}$ (Table B-1) is dominantly bicarbonate and $[CO_3^{2-}]$ is about 10^{-5}M. Log Ksp of SrCO$_3$ is -9.6 which means the solubility of Sr is about 2×10^{-6}gm/gm.

C: We set the solubility limit of ^{14}C at a level consistent with the concentration of HCO$_3^-$ in J-13 water (~26 ppm carbon).

B.3 Radionuclide Sorption Ratios

The ranges of radionuclide distribution coefficients (Rd) used in our calculations are listed in Table 4. The values were chosen after a review of the published experimental studies that were conducted at Los Alamos National Laboratories through June, 1981. (5-10).

Rd values from batch experiments obtained under the following conditions were included in the ranges shown in Table 4.

temperature = 22°C
solid: solution ratio = 1:20
atmosphere = oxidizing
particle size = 106-500 microns
water = J-13 water pre-equilibrated with the rock sample.
rocks = samples from UE25a-1, G-1 and J-13 drill holes.

Parametric studies by L.A.N.L. scientists (5-10) suggest that the measured Rd values are dependent upon all of the parameters listed above. The conservatism of the data collected under these experimental conditions with respect to natural conditions expected at the tuff repository site is described in Table B-2.

For several elements, Rd values obtained under these experimental conditions can vary up to 3 orders of magnitude between samples of the same bulk mineralogy. The measured Rd value are strongly dependent upon the abundance of minor minerals such as montmorillonite, the duration of the experiment and upon the method used to measure the concentration of the sorbed radionuclide. Values obtained from desorption experiments are almost always significantly higher than those obtained from sorption experiments. The data ranges in Table 4 bracket the highest average Rd values obtained from desorption experiments and the lowest average sorption Rd value. Each average value that was considered is the mean Rd value for a single rock sample for several experiments which lasted from 3 to 12 weeks.

TABLE B-2

CONSERVATISM[1] OF LABORATORY
DETERMINATIONS OF Rd (L.A.N.L.)

PARAMETER	ELEMENT								
	Pu	Am	U	Sr	Cs	Ba	Ce	Eu	Tc
Radionuclide Concentration	*0	ND	ND	-	-	-	ND	0	ND
Solid/Solution Ratio	ND	ND	ND	-0	-0	-	-	-	ND
Ionic Strength	ND	ND	ND	-*	-*	-*	-*	-*	ND
Temperature	ND	0	+	+	+	+	*	*	ND
Particle Size	-0	+0	+0	+0*	+0*	+0*	0	0	ND
TYPE EXPERIMENT:									
Batch vs. Column	ND	ND	-*	-	-	-	-*	ND	ND
Eh (Atmosphere)	+	0	+	0	0	0	0	0	+

KEY: + Conservative
      - Not conservative
      0 Little effect
      * Inconclusive or interaction effects
    ND Not determined

[1]   Assuming the following experimental conditions:

T = 220°C	Atmospheric conditions	J-13 water
Solid : Solution = 1:20	106-500 m particle size	
Batch experiment	element-specific concentration	

date May 13, 1982

to M. D. Siegel - 4413

Ken

from K. L. Erickson - 5843

subject Approximations for Adapting One-Dimensional Porous Media
Radionuclide Transport Models to the Analysis of Transport
in Jointed Porous Rock

This memorandum describes the basic ideas and results given
in the informal notes provided you on 2 April 1982 and subse-
quently discussed by us on 20 and 21 April. The following
remarks are confined to transport through a s'   'e, uniform
jointed geologic medium. However, additional   .yses since
our meeting of 20 April indicate that similar .esults probably
can be proved for a series of dissimilar jointed media.

Consider a region of jointed porous rock through which fluid
flow occurs primarily in the joints and convective radionuclide
transport in the porous matrix of the rock is negligible. Let
the joints be linear, have rectangular cross-sections of
approximately constant and uniform dimensions, have continuous
physical and chemical properties, and be such that fluid flow
is essentially one-dimensional with uniform average velocity
v. Let the porous matrix be fully saturated, and let radio-
nuclide retardation (relative to convective fluid flow in the
joints) result from molecular diffusion in the pore water and
simultaneous sorption by the solid phases. Furthermore, let
the regions of porous rock bounded by the joints have approxi-
mately uniform shape and volume V_p. In the paragraphs below,
criteria are developed for determining when transport in such
jointed media can be approximated as transport through an
equivalent porous medium whose porosity is defined by joint
aperture, frequency, and orientation. Then, the appropriate
expression is defined for the retardation factor R to be used
in such equivalent one-dimensional porous media models having
the form

$$\frac{\partial C}{\partial t} + \frac{v}{R} \frac{\partial C}{\partial z} = \text{dispersion and decay terms} \tag{1}$$

where C is the radionuclide concentration (assumed cross-
sectionally uniform) in the flowing fluid in the joints; t is
time, and z is the coordinate in the direction of fluid motion.

For a uniform region of jointed porous rock, as described
above, assume: (1) fluid flow is laminar and velocity pro-
files can be replaced by the average velocity; (2) joint
apertures are sufficiently small so that fluid-phase radio-
nuclide diffusion perpendicular to the joint walls can be
approximated as a quasi-steady-state process and represented
by a linear-driving-force expression; (3) local sorption
equilibrium exists at the interface between flowing fluid and
bulk rock and between pore water and solid phases of the porous
matrix; (4) sorption of radionuclides results from a reversible
process such as adsorption or ion exchange; (5) solution-phase
radionuclide concentrations are due only to dissolved species
and are sufficiently dilute to be within the linear region of
the sorption isotherm and sufficiently dilute for Fick's law
with constant diffusion coefficient to be a reasonable approxi-
mation; (6) effects due to competing chemical reactions and
surface diffusion are negligible, and (7) parameter values are
constant. Furthermore, initially assume that mass transfer by
dispersion in the direction of flow is small relative to that
by convection. Then for a radionuclide which is present in the
initial inventory but which is not subsequently produced as a
daughter product, transport is described by the following
equations:

(material balance for the fluid in the joint)

$$\frac{\partial C}{\partial t} + v \frac{\partial C}{\partial z} = - \frac{1}{m} \frac{\partial q}{\partial t} - \lambda C - \frac{\lambda}{m} q \tag{1}$$

(flux expression at interface between flowing fluid and bulk
rock)

$$\frac{\partial q}{\partial t} = \frac{1}{R_f} (C - q_s/\overline{K}) - \lambda q \tag{2}$$

(material balance for the porous rock)

$$\frac{\partial q_i}{\partial t} = D_e \nabla^2 q_i - \lambda q_i \tag{3}$$

where

$$q = \frac{1}{V_p} \int_{V_p} q_i \, dV_p \tag{4}$$

and where D_e is the effective radionuclide diffusion coefficient in the porous rock; $\bar{K}$ is the bulk sorption distribution coefficient between porous matrix and external solution; m is the void volume (based on joint aperture, frequency, and orientation) per unit volume of porous matrix; R_f is an effective interfacial resistance to mass transfer; q_i is the local concentration in the porous rock; q_s is the value of q_i at the interface between matrix and flowing fluid; λ is the radionuclide decay constant, and the Laplacian ∇^2 is defined in a coordinate system convenient for describing diffusion in the porous matrix.

Using the following initial and boundary conditions, Rosen (1952, 1954) solved Eqs. 1-4 for flow around spheres and $\lambda = 0$:

$$q_i(r,x,0) = 0 \quad \text{for} \quad 0 \leq r \leq b \quad , \quad x \geq 0 \tag{5}$$

$$u(0,\theta) = C(0,\theta)/C_o = \begin{cases} 0 & , \quad \theta = t \leq 0 \\ 1 & , \quad \theta = t > 0 \end{cases} \tag{6}$$

where r is the radial coordinate and b is the radius of the spheres. Erickson (1981) gives a similar solution for a fluid flowing through a single fracture between two parallel, semi-infinite plates in which radionuclide diffusion was primarily perpendicular to the fracture and limited to a finite penetration depth. By substituting the appropriate expression for m, that is $\varepsilon/(1 - \varepsilon)$, the solution for flow through a system of joints forming several continuous plate-like regions of porous matrix (see Fig. 1) is obtained from the single-fracture result.

The exact solutions for the spherical and plate-like geometries are in the form of infinite integrals requiring numerical evaluation. However, for sufficiently large values of z/v, the infinite integrals approach relatively simple asymptotic expressions. In particular, if R_f is very small so that the radionuclide concentration in the fluid in the joint is essentially cross-sectionally uniform, then for flow around spherical regions of porous matrix

$$C/C_o = \frac{1}{2}\left[1 + \text{erf}\left(\frac{3\sigma\theta/2 - \gamma x}{2(\gamma x/5)^{1/2}}\right)\right] \tag{7}$$

and for flow around plate-like regions

$$C/C_o = \frac{1}{2}\left[1 + \text{erf}\left(\frac{2\sigma\theta - \gamma x}{2(\gamma x/3)^{1/2}}\right)\right] \tag{8}$$

provided that the effective bed length γx is greater than 50. For spherical regions, $\sigma\theta = 2D_e(t - z/v)/b^2$, $\gamma x = 3D_e\bar{K}z/vmb^2$, and b is the radius of the spherical regions. For plate-like regions, $\sigma\theta = D_e(t - z/v)/2b^2$, $\gamma x = D_e\bar{K}z/vmb^2$, and b is now the half-thickness of the plate-like regions. A criterion for determining when radionuclide concentrations in the fluid in the fractures can be considered cross-sectionally uniform is developed after the following discussion regarding Eqs. 7 and 8.

In general, it was felt that a system of plate-like regions of porous rock might be more representative of actual systems. Therefore, the following discussion is based on Eq. 8, although similar considerations naturally apply to Eq. 7.

The right side of Eq. 8 is symmetrical about the value of $C/C_o = 0.5$. If for a given value of t, $t_{0.01}$ is defined as the elapsed time required for C/C_o to reach a value of 0.01, and $t_{0.5}$, $t_{0.99}$, and $\theta_{0.5}$ are defined analogously, then from Eq. 8 and appropriate values of the error function

$$\frac{t_{0.99} - t_{0.01}}{\theta_{0.5}} = \frac{6.6}{(3\gamma x)^{1/2}} \tag{9}$$

and for $\gamma x > 50$

$$\frac{t_{0.99} - t_{0.01}}{\theta_{0.5}} < 0.54 .$$

This implies that as γx becomes large, the spread in the break-through curve becomes small relative to the distance its midpoint has traveled, because the time interval by which the value of $C/C_o = 0.01$ precedes the value of $C/C_o = 0.5$ and the interval by which the value of $C/C_o = 0.99$ trails become small relative to $\theta_{0.5}$ or $(t_{0.5} - z/v)$. For example, when $\gamma x > 50$, the intervals are about twenty-five percent or less of $\theta_{0.5}$. Furthermore, from Eq. 8

$$t_{0.5} = (1 + \bar{K}/m)z/v \tag{10}$$

and

$$v_{0.5} = v/(1 + \bar{K}/m) . \tag{11}$$

Therefore, as γx becomes large the solution to Eqs. 1-4 when $\lambda = 0$ approaches

$$C(z,t) = C[o,t - (1 + \overline{K}/m)z/v] \qquad (12)$$

which is of the same form as the solution to Eq. 1 when the decay and dispersion terms are negligible, that is

$$C(z,t) = C(o,t - Rz/v) \quad . \qquad (13)$$

For $\lambda > 0$ in Eqs. 1-4 and C_o replaced by $C_o e^{-\lambda t}$ in Eq. 6, the solution to Eqs. 1-4 is $e^{-\lambda t} U_o(z,t)$, where $U_o(z,t)$ is the solution for $\lambda = 0$. Similar remarks also apply to the solution of Eq. 1 in the form

$$\frac{\partial C}{\partial t} + \frac{v}{R} \frac{\partial C}{\partial z} = - \frac{\lambda}{R} C \qquad (14)$$

where $C(0,t > 0) = C_o e^{-\lambda t}$. Hence, for a radionuclide initially present in the inventory but not produced as a daughter by decay, Eqs. 1-4 ($\lambda \geq 0$) can be approximated by Eq. 1 if γx is suffi- ciently large; if R is taken as $(1 + \overline{K}/m)$, and if dispersion effects are small relative to convective transport. Due to the inherent uncertainties associated with analyses of radionuclide transport in geologic media, a twenty-five percent spread in the concentration profile about $t_{0.5}$ is probably not serious, and values of $\gamma x > 50$ are probably sufficiently large for Eqs. 1-4 to be approximated by Eq. 1.

For the simplest case of diffusion into a porous matrix in which the total porosity ϕ is available to the diffusion of radionuclides which is sufficiently well described by Eq. 3 using $D_e = D/\alpha^2 (1 + \rho K_D/\phi)$, the criterion $\gamma x > 50$ and the retardation factor $R = 1 + \overline{K}/m$ can be defined in terms of more fundamental parameters as follows

$$\gamma x = D_e \overline{K} z/vmb^2 > 50$$

or

$$\frac{z}{v} > 50 \frac{b^2 \alpha^2}{D\phi} \left(\frac{\epsilon}{1 - \epsilon} \right) \qquad (15)$$

and

$$R = 1 + \overline{K}/m = 1 + \left(\frac{1 - \epsilon}{\epsilon} \right) \left[\phi \left(1 + \frac{\rho}{\phi} K_D \right) \right] \qquad (16)$$

where D is the diffusion coefficient for the radionuclide in aqueous solution (assumed constant); K_D is the distribution coefficient for sorption equilibrium between pore water and solid phases of the matrix (units of ml/gm); α is a tortuosity factor for the matrix, and ρ is the bulk dry density of the matrix ($\rho = (1 - \phi)\rho_s$ where ρ_s is the average grain density of the matrix material).

The preceding development was based on the assumption that radionuclide concentrations in the flowing fluid were cross-sectional uniform. A criterion for the validity of that assumption is that the average fluid residence time in the joints is much greater than the characteristic time required for a concentration gradient to decay to near zero. The average fluid residence time in the fractures is z/v. Now, let H denote joint aperture, and assume that the characteristic decay time for a concentration gradient can be approximated by the equilibration time for a plane sheet of thickness H/2 and having one face maintained at a constant concentration. Then the characteristic decay time would be $H^2/4D$ (Crank, 1975), and the desired criterion is

$$z/v \gg H^2/4D \quad . \tag{17}$$

In summary, for a radionuclide which is initially present in the inventory and not subsequently produced by decay, transport through a single, uniform, jointed porous medium can be described approximately by Eq. 1 provided that

$$z/v \gg H^2/4D \tag{17}$$

and

$$z/v > 50 \, \frac{b^2\alpha^2}{D\phi} \left(\frac{\epsilon}{1 - \epsilon} \right) \tag{15}$$

The value for the retardation factor R in Eq. 1 is given by

$$R = 1 + \left(\frac{1 - \epsilon}{\epsilon} \right)\left[\phi\left(1 + \frac{\rho}{\phi} K_D \right)\right] \quad . \tag{16}$$

As given previously, b is the half-thickness for the plate-like regions between joints; D is the radionuclide diffusion coefficient (assumed constant) in aqueous solution; H is the joint aperture; K_D is the distribution coefficient for sorption equilibrium between pore water and solid phases of the porous

matrix; $\bar{K} = \phi(1 + \rho K_D/\phi)$; $m = \epsilon/(1 - \epsilon)$; v is the average fluid velocity in the joints; z is the spatial coordinate in the direction of bulk fluid motion; α is a tortuosity factor for the porous matrix; ϵ is the porosity associated with the joints; $\rho = (1 - \phi)\rho_s$ and is the bulk dry density of the porous matrix material; ρ_s is the average grain density of the matrix material, and ϕ is the porosity of the porous matrix.

However, it should be emphasized that the applicability of Eqs. 15-17 depends on how closely a real system is approximated by the ideal system and assumptions from which the equations were developed. In particular, the treatment given for diffusion of radionuclides into the porous matrix may not be adequate in certain situations, particularly if very "tight" porosity is involved.

REFERENCES

Crank, J., The Mathematics of Diffusion, 2nd ed., pp. 49-53, Clarendon Press, Oxford, 1975.

Erickson, K. L., A Fundamental Approach to the Analysis of Radionuclide Transport Resulting from Fluid Flow Through Jointed Media, SAND80-0457, Sandia National Laboratories, Albuquerque, NM, 87185.

Rosen, J. B., "Kinetics of a Fixed Bed System for Solid Diffusion into Spherical Particles," J. Chem. Phys., V. 20, 3 (1952).

Rosen, J. B., "General Numerical Solution for Solid Diffusion in Fixed Beds," Ind. and Eng. Chem., V. 46, 8 (1954).

KLE:5843:ls

Distribution:
4410   D. J. McCloskey
4413   M. S. Y. Chu
4413   R. M. Cranwell
4413   N. R. Ortiz
4413   R. E. Pepping
5840   N. J. Magnani
5843   C. J. M. Northrup
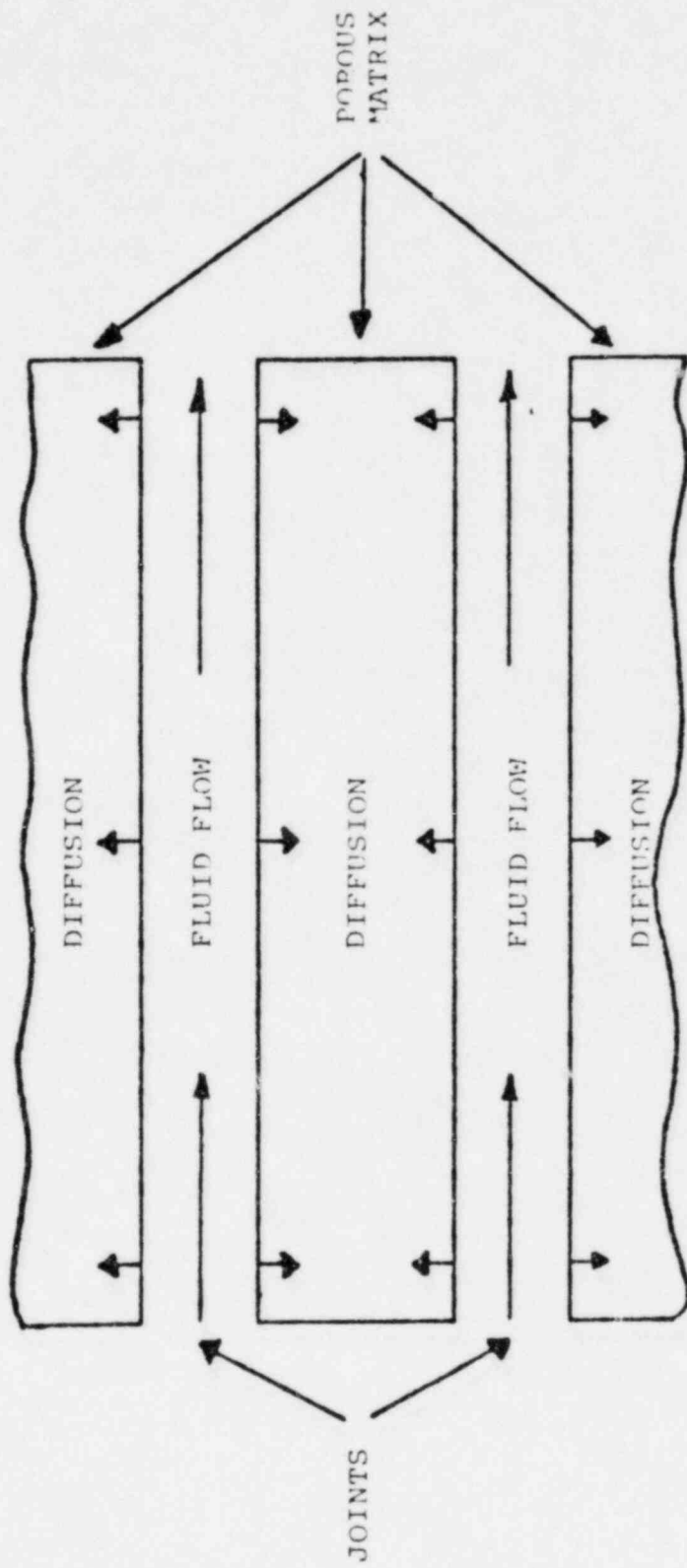5843   K. L. Erickson

Fig. 1. Schematic diagram of fluid flow through joints and diffusion into the porous matrix.

TO: Stewart Silling

FROM: Malcolm Siegel

RE: Calculation of Effective Retardation Factor ($\bar{R}$) for
         Matrix Diffusion

1. For retardation factor in NWFT/DVM runs use: ($\bar{R}$):

$$\bar{R} = 1 + \phi \cdot \left(\frac{1-\epsilon}{\epsilon} \right) \cdot \left(1 + \frac{\rho (1-\phi)}{\phi} \cdot K_D \right)$$

where:
    K_D = distribution coefficient in ml/gm
    ϕ = matrix porosity of unfractured blocks
    ρ = grain density of rock
    ϵ = fracture porosity = 2Nb for our system where
        N = fracture density; b = fracture aperture

2. This expression is good when the following criterion (1)
    holds:

$$z/v \geq 50 \cdot (1/N^2 D) \cdot (\alpha^2/\phi) \cdot (\epsilon/1-\epsilon) = \gamma x$$

where:
    D = ionic diffusion constant
    α = tortuosity
    z = path length in fractured media
    v = Darcy velocity ÷ fracture porosity

The criterion was evaluated for densely and moderately welded
tuff units, for individual beds as well as for the entire
welded tuff thickness. The maximum, median and minimum
values of the ranges used for the LHS input variables were
used to evaluate the expression (γx).

ATTACHMENT 1

	γx max	γx min	γx median
z	200 ft	200 ft	100 ft
ϵ	6.4×10^{-3}	8.8×10^{-6}	1.3×10^{-4}
ϕ	0.03	0.10	0.06
N	6.5 ft^{-1}	0.27 ft^{-1}	1.6 ft^{-1}
K	60 ft/day	4×10^{-5} ft/day	4.2 ft/day
i	4×10^{-2}	1×10^{-2}	2×10^{-2}
v	375 ft/day	0.045 ft/day	0.646 ft/day
z/v	0.533 day	4.4×10^{3} day	155 day
γx	0.19 day	0.045 day	0.031 day

where:

i = vertical hydraulic gradient

$D = 10^{-5}$ cm^2/sec = 3.39×10^{-1} ft^2/yr

$\alpha = 1.0$

K = hydraulic conductivity in LHS range for densely welded units

$v = iK/\epsilon$

It can be seen from these calculations that the criterion $z/v \geq \gamma x$ holds for the conditions encountered at the tuff site.

References:

(1) Erickson, K. L., 1981, A Fundamental Approach to the Analysis of Radionuclide Transport Resulting from Fluid Flow through Jointed Media, SAND80-0457. (See p. 19-2 and work backwards. See also reference 14 in his bibliography.)

REFERENCES

1. Spengler, R. W., Muller, D. C., and Livermore, R. B.
    1979, Preliminary Report on the Geology and Geophysics at
    Drill Hole UE25a-1 Yucca Mountain, Nevada Test Site.
    U. S. G. S. Open File Report 79-1244, 43p.

2. Sykes, M. L., Heiken, G. H., and Smyth, J. R. 1979,
    Mineralogy and Petrology of Tuff Units from the UE25a-1
    Drill Site, Yucca Mountain, Nevada: Los Alamos National
    Laboratory. LA-8139-MS, 76p.

3. Johnstone, J. K., and Wolfsberg, K. eds. 1980, Evalua-
    tion of Tuff as a Medium for a Nuclear Waste Repository:
    an Interim Status Report on the Properties of Tuff, Sandia
    National Laboratories Report; SAND80-1464, 142p.

4. Winograd, I. J. and Thordarson, W. 1975, Hydrogeologic
    and Hydrochemical Framework, South-Central Great Basin,
    Nevada-California, with Special Reference to the Nevada
    Test Site, U. S. G. S. Prof. Pap. 712-C, 126p.

5. Wolfsberg, K. 1978, Sorption-Desorption Studies of Nevada
    Test Site Alluvium and Leaching Studies of Nuclear Test
    Debris, Los Alamos Scientific Laboratory Report
    LA-7216-MS, 33p.

6. Wolfsberg, K., Daynurst, B. P., et al. 1979, Sorption-
    Desorption Studies on Tuff I. Initial studies with
    samples from the J-13 Drill Site, Jackass Flats, Nevada,
    Los Alamos Scientific Laboratory Report LA--7480-MS, 60p.

7. Vine, E. N., Aguilar, R. D., et al. 1980, Sorption-
    Desorption Studies on Tuff II. A continuation of studies
    with samples from Jackass Flats, Nevada, and initial
    studies with samples from Yucca Mountain, Nevada, Los
    Alamos Scientific Laboratory Report LA-8110-MS, 75p.

8. Erdal, B. R., Daniels, W. R. and Wolfsberg, K., eds. 1981,
    Research and Development related to Nevada Nuclear Waste
    Storage Investigations, January 1 - March 31, 1981, Los
    Alamos Scientific Laboratories Report LA-8847-PR.

9. Wolfsberg, K., Aguilar, R. D., et. al. 1981, Sorption-Desorption Studies on Tuff III. A continuation of studies with samples from Jackass Flats and Yucca Mountian, Nevada, Los Alamos National Laboratory Report LA-8747-MS.

10. Erdal, B. R., Daniels, W. R., Vaniman, D. T., and Wolfsberg, K. 1981, Research and Development related to the Nevada Nuclear Waste Storage Investigations, April 1 - June 30, 1981, Los Alamos National Laboratory Report LA-8959-PR, 65p.

11. Guzowski, R. V., Nimick, F. B., and Muller, A. B. 1982, Repository Site Definition in Basalt: Pasco Basin, Washington, SAND81-2088, NUREG/CR-2352, Sandia National Laboratories, 88p.

12. Ogard, A. E. 1982, Personal communication.

13. Nimick, F. 1982, letter report on solubilities of radio-nuclides in basalt. Sandia National Laboratories.

14. Rai, D and Serne, R. J. 1978, Solid Phases and Solution Species of Different Elements in Geologic Environments, Battlelle, Pacific Northwest Laboratories Report PNL-2651, 140p.

15. Wood, B. J. and Rai, Dhanpat 1981, Nuclear Waste Disposal: Actinide Migration from Geologic Repositories, Battelle, Pacific Northwest Laboratories Report PNL-SA-9549, 33p.

16. Muller, A. B., Finley, N. C., Pearson, F. J. 1981, Geo-chemical Parameters used in the Bedded Salt Reference Repository Risk Assessments Methodology, Sandia National Laboratories, SAND81-0557, NUREG/CR-1996, 86p.

17. Campbell, J. E., Longsine, D. E. and Cranwell, R. M., Risk Methodology for Geologic Disposal of Radioactive Waste: The NWFT/DVM Computer Code Users Manual, SAND81-0886, Sandia National Laboratories, November 1981.

18. Iman, R. L., Davenport, J. M. and Zeigler, D. M., *Latin Hypercube Sampling (Program Users Guide)*, SAND79-1473, Sandia National Laboratories, January, 1980.

19. Environmental Protection Agency, 40CFR191, Draft 19, *Federal Register*, March 19, 1981.

20. Cranwell, R. M. et. al. *Risk Methodology for Geologic Disposal of Radioactive Waste: Final Report*, SAND81-2573, NUREG/CR-2452, Sandia National Laboratories, to be published.

21. Rush, F. E. 1970, Regional ground-water systems in the Nevada Test Site area, Nye, Lincoln, and Clark Counties, Nevada: Nevada Department of Conservation and Natural Resources, Water Resources - Reconnaissance Series Report 54, 25p.

22. Reade, M. T. 1982, letter report on geology and hydrology of the Nevada Test Site. C. G. S. Inc.

23. Longsine, D. 1982, Unpublished manuscript.

24. Freeze, R. A. and Cherry, J. A. 1979, *Groundwater*, Prentice-Hall Inc., Englewood Cliffs, N.J., p. 74.

25. Guzowski, R. 1982, oral presentation for NRC on Hydrology at Nevada Test Site.

26. Merkin, J. H. 1979, Free Convection Boundary Layers on Axi-Symmetric and Two-Dimensional Bodies at Arbitrary Snape in a Saturated Porous Medium, Int. J. Heat Mass Transfer, 22:1461-1462.

27. Interim Reference Repository conditions for spent fuel and commercial high level nuclear waste repositories in Tuff, Sept. 1981. Battelle Project Management Division (ONWI) NWTS-12.

28. Rush, G. 1982, Personal Communication.

29. White, A. F., Claassen, H. C. and Benson, L. V. 1980, The Effect of Dissolution of Volcanic Glass on the Water Chemistry in a Tuffaceous Aquifer, Rainier Mesa, Nevada, Geological Survey Water-Supply Paper 1535-Q, 34p.

30. Winograd, I. J. and Robertson, F. N. 1982, Deep Oxygenated Ground Water Anomaly or Common Occurrence?, Science, in press.

31. Erdal, B. 1982, NRC field trip to NTS and project reviews.

32. Serne, J. 1982, personal communication.

33. Baes, C. F. and Mesmer, R. E., 1976. The Hydrolysis of Cations, Wiley Interscience, John Wiley and Sons, New York, N. Y., p.166.